Corvus: Urban Air Mobility Solutions for Package Delivery

A Technical Report submitted to the Department of Mechanical and Aerospace Engineering

Presented to the Faculty of the School of Engineering and Applied Science
University of Virginia • Charlottesville, Virginia

In Partial Fulfillment of the Requirements for the Degree
Bachelor of Science, School of Engineering

Brett A. Brunsink

Spring, 2020

Technical Project Team Members

David Normansell	Daniel Choi	Joseff Medina
Cristhian Vasquez	Derrick Devairakkam	Justin Robinson
Henry Smith III	Gino Giansante	Philip Hays
Timothy Mather	JD Parker	Alejandro Britos

On my honor as a University Student, I have neither given nor received unauthorized aid on this assignment as defined by the Honor Guidelines for Thesis-Related Assignment

James McDaniel, Department of Mechanical and Aerospace Engineering

Corvus

An Advanced, Tilt-Wing, Autonomous, Electric Drone Delivery Vehicle and Business Model

University of Virginia Aircraft Design Team

James C. McDaniel
Faculty Advisor

UNIVERSITY of VIRGINIA | SCHOOL of ENGINEERING & APPLIED SCIENCE

Table of Contents

Abstract

Unmanned Aerial Vehicles (UAVs) are expanding in prevalence, finding use in daily applications. Moving beyond their introduction as simplistic RC hobby aircraft, UAVs are rapidly being deployed across the civilian and military sectors. A common example of a civilian application is UAV "camera drones." In contrast, military UAVs fill expanded, versatile roles, to include reconnaissance and kinetic combat applications. These purposes of use often require military UAVs to be much larger than commercial products in order to accommodate duration of flight and equipment requirements. These added specifications thereby make them impractical and/or unfeasible for use within civilian sectors.

The entrepreneurial spirit and push for innovations across civilian markets are creating demands for UAV advancements that accommodate new applications. This demand includes delivery service providers who are particularly interested in using UAVs to expedite and simplify the logistics of delivering goods. To meet the growing call for UAVs to fill newly identified service roles within commercial industries, more robust UAVs, that break free of current miniature hobbyist roles, are required. The pioneering enhancements of quad-rotors and small-scale airframes are integral requirements in fulfilling UAVs promise and use.

The fully autonomous Corvus drone is a UAV design capable of meeting or exceeding the needs of logistics companies in drone package delivery applications. Corvus utilizes a cutting-edge tandem tilt-wing design in order to maximize its performance potential in a variety of situations, including adverse weather conditions. In addition, Corvus is capable of performing two or more consecutive package deliveries, all without any human interaction. Corvus is the solution to a safe, efficient, fast, and reliable autonomous drone delivery system.

1. Configuration Highlights

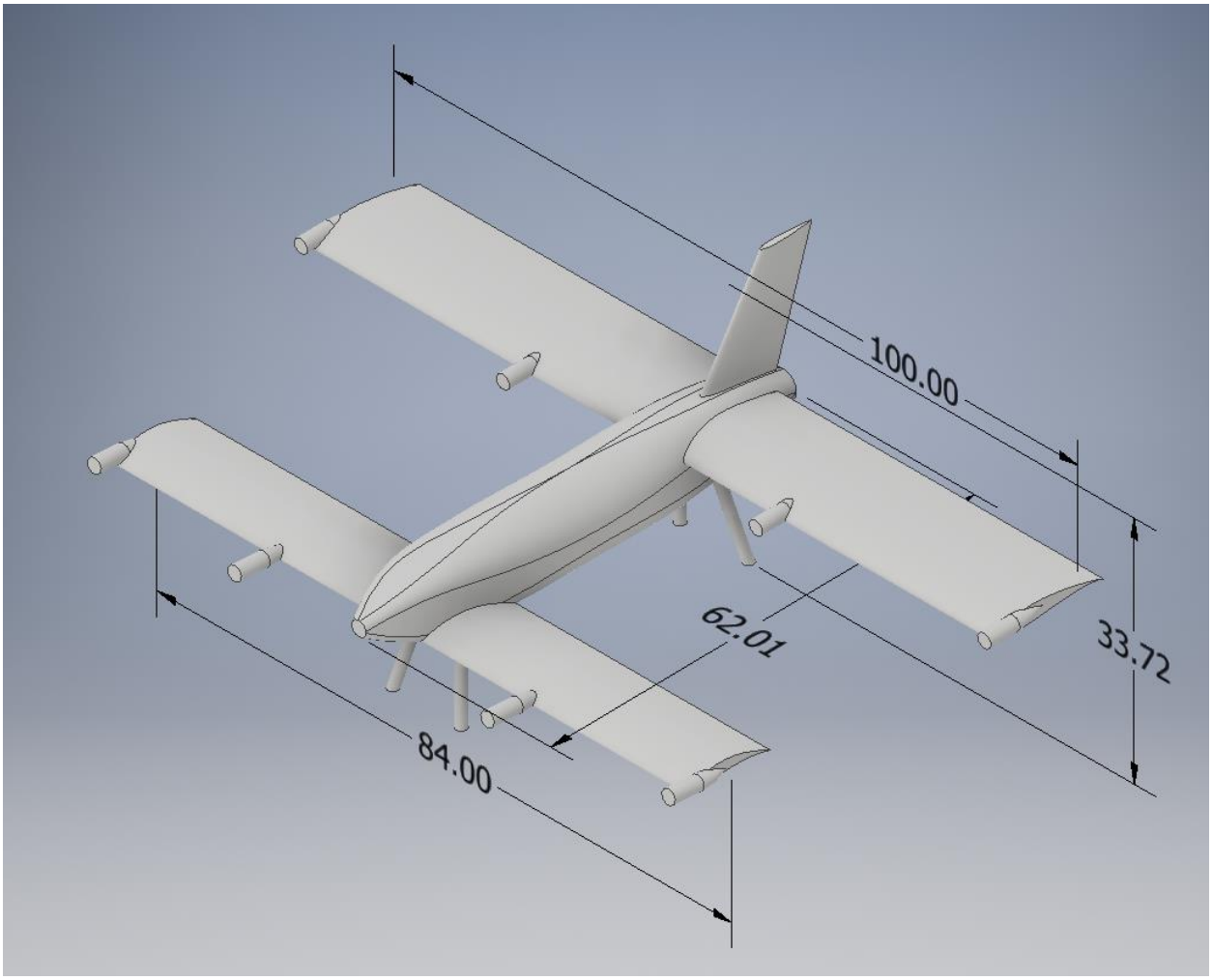

Aerodynamic Characteristics	
Front Airfoil	CH 10-48-13
Rear Airfoil	FX 63-137
Front Chord	12 inches
Rear Chord	16 inches
Front Span	84 inches
Rear Span	100 inches
Front incidence angle	0.5 degrees

Rear incidence angle	-0.8 degrees
Vertical tail height	16 inches
Vertical tail area	302 in^2
Fuselage length	62 inches
Fuselage volume	4100 in^3

Propulsion Characteristics	
Motors	Eight MAD M10 IPE 150KV motors
ESCs	80 amps
Propeller Diameter	22 inches
Propeller Pitch	Variable (operating range: 10-20 inches)
Motor Thrust	Up to 194 pounds (24.25 per motor)
Maximum Throttle Power Consumption (100%)	21.184 kilowatts (2.648 per motor)
Cruise Throttle Power Consumption (45%)	2.4272 kilowatts (0.3034 per motor)

Performance Characteristics	
Empty Weight	98 lb
Loaded Weight	103 lb
Endurance	45.9 min
Range (1 battery charge)	30 miles
Cruise Speed	70 mph
Max Rate of Climb (Sea Level)	6025 ft/min

Cost Characteristics	
Development Cost	$2,838,607
Facility Costs (average per distribution center)	$6,000,000
Operational Costs (per drone, per year)	$291,500
Unit Cost	$10,033

2. Introduction

2.1 Mission Requirements

This year's NASA design challenge was to design a safe, low-noise, profitable unmanned aerial system (UAS or drone) to deliver five pound packages across short distances. Also, the ground infrastructure to facilitate autonomous delivery are included in the design. The primary design requirements here are the safety, reliability, profitability, and performance of the UAS. Other aspects that must be met are noise and operations of the drone system (NASA, 2019). There are no aircraft on the market currently that fulfill the full breadth of design requirements, though there are many upcoming drones such as the WingCopter 178HL (Wing, 2020) that fulfill several requirements.

Table 1: Design requirements for 2019-20 ARMD Challenge (NASA, 2019)

NASA Design Challenge Requirements
Takeoff and land in 25 by 50 ft. area
Climb to 400 ft. within 1 mile of takeoff
Land at sites up to 8000 ft. above sea level

Fly in winds up to 20 knots
Carry a 6x6x6 in. package weighing up to 5 lb.
Conduct 2 trips over a 10 mi. radius autonomously, each trip in under 20 minutes
“Detect and Avoid” system and integration with FAA UTM system
Delivery system throughput of 1 package every 2 minutes
Collision with a pedestrian must not be fatal
“Acceptable” noise level

2.2 Drones for Delivery

The UVA 2019-20 aircraft design team proposes the *Corvus* to meet the design challenge requirements. This UAS incorporates novel autonomous algorithms in a tilt-wing airframe that enables vertical take off and landing (VTOL), and traditional cruise flight. The entire system is powered by advanced Lithium-Ion batteries for affordability and sustainability.

2.3 Design Methodology

This design challenge was undertaken by a team of thirteen 4th-year aerospace engineering students from the University of Virginia. To facilitate the design process, the students split into three teams each specializing in a different major aspect of design. These teams focused on aerodynamics, propulsion, and performance, with further specialization into structure, power, and propulsion, respectively.

The team began by brainstorming ideas from prior art and individual ideas. Initial brainstorming yielded over a dozen concepts. Because of the temporal and computational cost of running CFD analysis on each design, the team reduced the number of designs to 3, in the major categories of Lift/Cruise, Tailsitter, and Tilt Wing designs. Several full group discussions were

used to choose components for each of these major categories, before each design was modeled using Autodesk Inventor and analyzed using Autodesk CFD. The resulting lift and drag figures, along with other qualitative assessments were used in a design matrix to choose which of the major configurations was the best. Metrics to compare the designs included weight, projected horizontal performance, vertical performance, and more. All the metrics were weighted on a scale of one to three, with three being of high importance and one being of lower importance. The class then used the calculated numbers to rank the designs in the quantitative categories, such as horizontal performance, and had a large discussion to rank the qualitative components of each design. The results of this process can be seen in Figure 1. The Tailsitter and the Tiltwing tied, at which point the Lift/cruise was removed from scoring and the rankings were recalculated. A tilt wing configuration was thus chosen.

The team recognized that the propellers would significantly alter the aerodynamics of Corvus, but due to lack of resources was unable to simulate the drone with the propellers. The assumption was that the airframe aerodynamics would still be relevant even with the propellers disturbing the flow. Specific lift and drag values may be inaccurate, but across iterations and configurations, improvements to lift and drag on the airframe could be used to decide which design choices were best.

Following the selection of a tilt wing configuration, the teams worked out all the specific parameters of the design. The aerodynamics team sized the drone and selected appropriate airfoils to generate enough lift, the performance team calculated power requirements and designed safety features, and the propulsion team selected motors, propellers, and controllers. Full specification of the UAS follows in this report.

			Revised	Revised			
Indice of Performance	Measurement	Weighting (1-3)	Tiltwing	Tailsitter	Tiltwing	Tailsitter	Lift cruise
Vertical	power req. for 1.5 L/W	2	1	0	1	0	0.5
Cruise	drag at 60 mph with props	3	1	0	1	0.5	0
transition	qualitative	3	0	1	0	0.5	1
package handling		1	1	0	1	0.5	0
power consumption		3					
loudness	# size, and rpm of props	1	0	1	0	1	0.5
Redundancy	# of props + configuration	2	1	0	1	0.5	0
detect and avoid	maneuverability	2	0	1	0	0.5	1
survivability		2	1	0	1	0.5	0
maintenance		1	0	1	0	1	0.5
danger to people		3	1	1	0.5	0.5	1
weight		3	1	0	1	0.5	0
complexity	qualitative	3	0	1	0	1	0.5
Total		17	16	13	14.5	14.5	11.5

Figure 1: Design Matrix

2.4 Software

Table 2 shows the various software used throughout the design process to refine the design and predict performance.

Table 2: Software used during design phase of drone

Software	**Team**	**Use**
Autodesk CFD	Aerodynamics	Analyzing the lift and drag of the drone
Autodesk Inventor	All	Modeling the drone
MATLAB	Aerodynamics	Stability assessments, fast lift prediction from design changes
MotoCalc	Propulsion	Predicted motor and propeller performance

3. Design Summary

3.1 Configuration Aerodynamics

As stated in the previous section, a tandem/tilt wing design was selected as the final design configuration. The tandem wing design allowed the wing sizes to be smaller, due to the fact that both wings produced lift. However, the wings had to be placed in locations on the fuselage so as to diminish flow perturbation on the rear wing due to the downwash effects and swirls coming from the front wing. Any flow disturbances from the front wing would reduce and alter the efficiency of the rear wing. As a result, the drone is designed with the rear wing placed higher on the fuselage and the front wing placed lower, with vertical spacing between the two wings so as to reduce the interactions of flow. Table 3 shows the total lift and drag of the drone configuration.

Table 3: Cruise Aerodynamic Forces

Cruise Summary (4.06 degrees)	
Total Lift	107.7 lbf
Total Drag	35 lbf
Front Wing Lift	56.1 lbf
Rear Wing Lift	44.2 lbf

3.2 Airfoil Design/Selection

A tandem wing design required specific aerodynamic aspects of its front and rear wings. In general, any pair of tandem wings must be selected so that the front wing has a lower stall angle, and the rear wing has a lower zero lift angle. This is a safety requirement to ensure that the aircraft does not achieve flight conditions from which it is unable to recover from a stall or dive [Lennon, 1996]. If the rear wing stalls before the front wing in the act of climbing, then the rear

of the aircraft will inevitably fall out from underneath the aircraft, resulting in a severe stall. If the front wing arrives at zero lift before the rear wing during cruise or a dive, then the front wing will pull the front of the aircraft down, resulting in a recoverable dive.

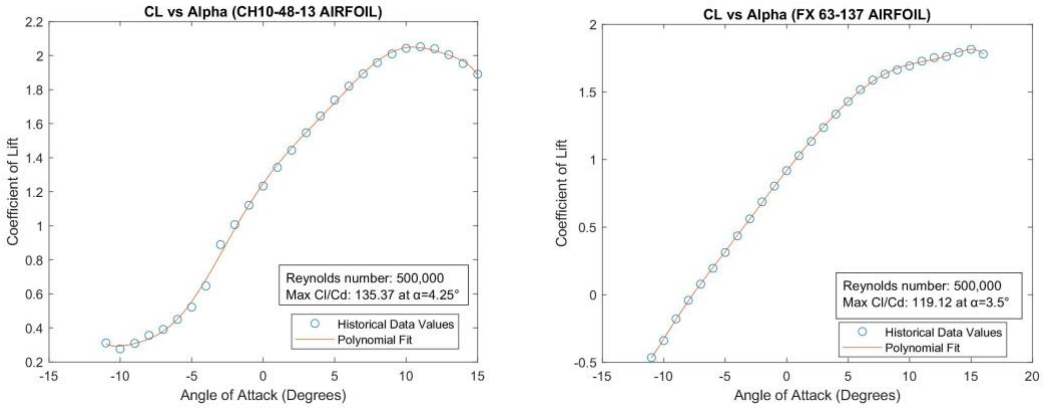

Figure 2: Lift-curve slopes of the fore (CH10) and aft (FX 63) wings

Figure 2 displays the lift-curve slopes of the selected airfoils. With the CH10 airfoil selected as the front wing and the FX 63 airfoil selected as the rear wing, the conditions of stall angle and zero-lift angle were satisfied for the tandem wing configuration. It should be noted that all airfoil data were selected at a Reynolds number of 500,000, as our drone flies at approximately the same value. In addition, the wings are configured to fly close to the angles of max Cl/Cd, so as to maximize the efficiency of each wing.

3.3 Wing Choice and Sizing

In the wing selection process, the first condition to satisfy was selecting a pair of airfoils that would produce an evenly-distributed lift to support the UAV in cruise conditions. The purpose of evenly-distributed lift between the front and the back wing in cruise conditions was to have a C.G. near the geometric center of the configuration so that the UAV would be stable during VTOL. The following airfoils were analyzed and simulated in Autodesk CFD.

Table 4: Airfoil Selection

Airfoil Name	Location	Zero-Lift Angle of Attack (degrees)	Lift Slope (1/deg)	Stall Angle (degrees)	Moment Coefficient (from CFD)
FX-74Cl5-140	Back	-10.93	0.1103	14	-0.2307
Eppler 214	Front	-4.5	0.108	18	-0.0787
Selig 1223	Back	-7	0.1064	17	-0.249
Eppler 214	Front	-4.5	0.108	18	-0.0787
Selig S1210	N/A	-10.14	0.1071	11.9	N/A
CH-10-48-13	Front	-11	0.0945	15	-0.2691
FX 63-137(B)	Back	-7.75	0.1025	17.5	-0.1899
GOE 227	N/A	-9.74	0.0997	7.8	N/A

From table 4, the two airfoils highlighted in red (FX-63 and CH-10) were selected after an iterative process of varying airfoil profiles, wing size, wing location, and angle of incidence. The iterative process of analyzing different wing characteristics sought to satisfy the three following conditions: enough lift to support UAV, longitudinal stability, and C.G. at least 24 inches from the tip of the fuselage.

3.4 Stability Assessments

Our team designed a statically stable configuration at cruise since most of the mission profile will be flying at cruise conditions. To obtain the pitching moment of the entire UAV, a MATLAB script was developed (See appendix A). In the code, some assumptions and definitions are presented to calculate and derive the pitching moment about the UAV's C.G. The following graph summarizes our results.

Summary	
Loaded Weight	103 lbs
Empty C.G. Location	25 in
Loaded C.G. Location	25 in
Neutral Point Location	27.75 in
Trim Angle	4 Degrees

Notes

- All distances are measured from the tip of the nose
- Total length of the fuselage is 62 in
- Distances are rounded to the closest ¼ of an inch

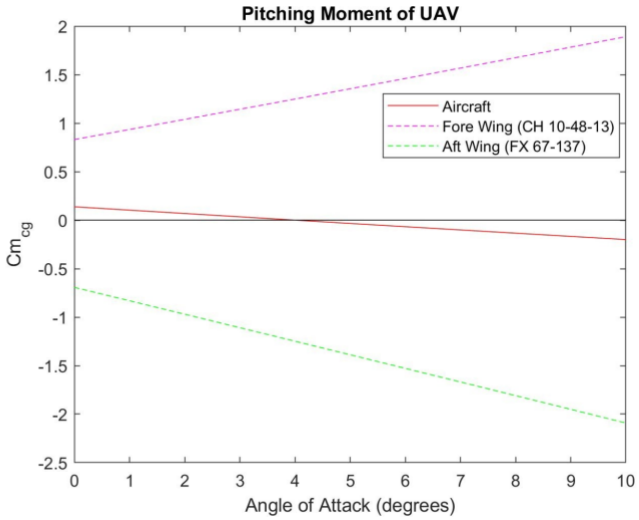

Figure 3: Static Stability Assessment of UAV

The curve from the graph shows that as the angle of attack increases, the resulting pitching moment acts in a direction to decrease the angle of attack; therefore, our configuration is statically pitch stable.

3.5 Structure, Placement of Components

In order to meet the various specifications required by the design challenge, various internal components were required. The items needing to be considered are a package, batteries, two computing units, wing spars, and parachutes in the case of total system failure. In addition, the required structure to obtain flight also contributed to the weight total, and such items include the wings, fuselage, landing struts, propellers and motors. Many factors affected the placement of items within the fuselage, mainly the location of the center of gravity, ease of access and safety. For optimal VTOL performance the center of gravity would be in the geometrical center; however, for the aircraft to be stable during cruise flight, the center of gravity needs to be in front of the neutral point.

These challenges required many iterations throughout the design process as the overall configuration of the drone was changed. After the performance analysis, the neutral point is located approximately 27 inches from the tip of the drone (4 inches ahead of the geometrical center) and thus leaving a tight window between the neutral point and the front wing. This left a target center of gravity located in the neighborhood of 25 inches from the tip. The next thing to consider was how the drone would interact with the ground system and how the package and batteries would be changed. Because the package is the only internal item that would not be inside the fuselage for the duration of flight, it was placed over the center of gravity to maintain constant performance when the drone is loaded or unloaded. Since the package and batteries must be loaded and unloaded from the bottom autonomously, our team designed their distribution without restricting the package from beneath. Figure 4 displays the location of all the components within the fuselage. Top and side views are in Appendix B along with the table of weights and locations of all the specific components.

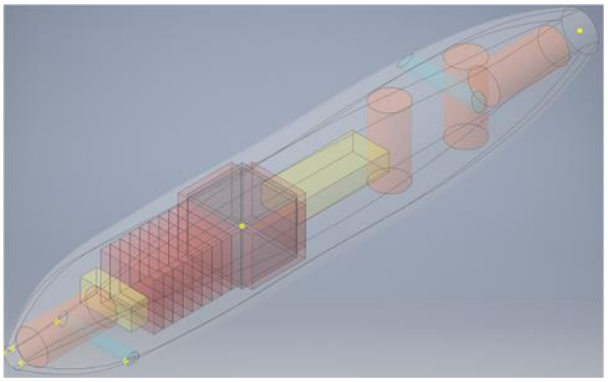

Isometric view of interior of the fuselage.
Blue: Wing spars
Gray: Package
Orange: Parachutes
Red: Batteries
Yellow: Computing units

Figure 4: Internal structure of UAS

3.6 Material Selection

Four different materials were selected for the UAV structure. For the fuselage, our team decided to use a thin carbon-fiber monocoque (0.1 in thick) due to its low weight and strength properties. For the wings, our team used extruded polystyrene foam due to its low price, light weight, ductility, and popularity with the model airplane community (Depron Foam, n.d.). See Appendix C for a complete material specification of the foam. The leading edge of all wings was reinforced with carbon fiber to prevent them from breaking under extreme conditions. In addition, the fore and aft wings were reinforced with aluminum spars to support the lift and drag forces (See Appendix D for a stress analysis). Lastly, for the landing gear, our team decided to use aluminum because of its strength, light weight, and low cost. The landing gear was designed as hollow cylinders to reduce weight, while retaining most of the structural properties.

3.7 Control

Roll

The UAV has ailerons on both front and rear wings for roll maneuvers. The front aileron has slightly more area, to account for the fact that the back wings are further from the CG in the longitudinal direction and the lateral direction. The back ailerons therefore have a greater moment arm in both pitch and yaw directions, so the front aileron area is greater to account for this difference. Unbalanced moments would create undesirable control effects, so they have been avoided. Figure 5 shows the balanced aileron sizing.

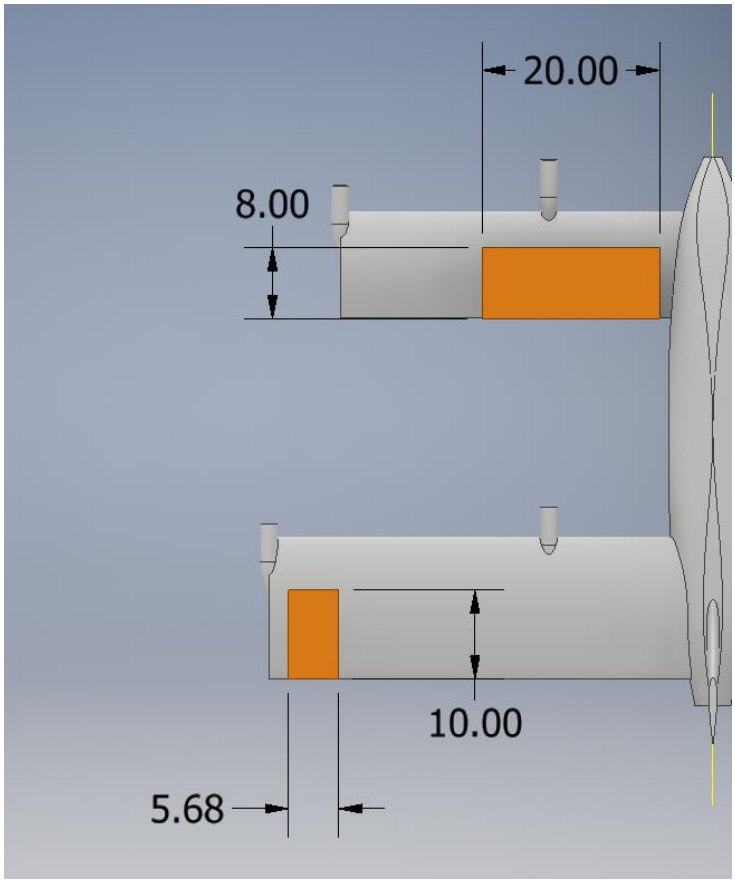

Figure 5: Ailerons sized to create equal moments around the CG

Pitch

The UAV uses its tilting wings and variable motor thrust to control its pitch. A pitch up maneuver is done by pitching up the front wing and pitching down the rear wing, or by increasing front wing motor thrust. A pitch down maneuver is the opposite process.

Yaw

The UAV uses a vertical stabilator and variable motor thrust to control its yaw. The airfoil used for the vertical stabilator was a NACA 0015. The vertical stabilizer was sized to permit an engine out condition of the outer rear engine while maintaining forward flight (see appendix E). In actuality, the drone is capable of flying with only half of the motors, so long as

the motors are in a symmetric arrangement, so the more effective engine out procedure is simply to switch to a different pair of motors and continue flying. The vertical tail can also be used for simple yawing maneuvers. An alternate option is varying the left/right balance of motor thrust to accomplish a yawing maneuver.

4. Performance Assessment

4.1 Mission Profile

Takeoff and Transition

The UAV will perform as a vertical takeoff and landing (VTOL) vehicle. The drone will take off in the vertical configuration with both wings pointed upwards and each of the eight motors thrusting downwards. Each motor will be set at the 90% thrust setting producing a force where L/W = 1.5. (See table 5) At 90 degrees, the vehicle will vertically climb to a minimum safe height that is determined on a case by case basis in order to avoid common obstacles found below this height.

Table 5: Transition Analysis

Wing's Angle of Attack (degrees)	Vertical Thrust (lbf)	Horizontal Thrust (lbf)	Coefficient of Drag	Maximum Velocity Forward (mph)
90	175	0	N/A	N/A
60	151.5	87.5	1.21	53
45	123.7	123.7	1.1	69
35	100.4	143.4	0.92	78
15	45	169.03	0.42	125

Since the complexity of the transition phase is beyond our CFD simulation capacities, a discrete set of angles was considered between VTOL and Cruise. Table 5 presents those results. The wings stall at 15 degrees; therefore, our team assumed that only the vertical thrust component of the UAV acts against the weight between 90 and 15 degrees angles of attack. (CFD shows that some lift is produced between 90 and 15 degrees; however, that lift is ignored since it cannot be predicted accurately) Below 15 degrees, the UAV wings produce enough lift to support the aircraft as long as the airspeed is greater than 47 mph. Moreover, from the results of Table 5, our team found out that between 35 and 15 degrees angle of attack, the vertical component of thrust is not enough to support the UAV; however, this uncovering can be neglected since it occurs for only 0.25 seconds (time that it takes the servos to rotate the wings 20 degrees) Now, another important result from table 5 is that the UAV can achieve the required velocity of 47 mph at any angle of attack less than 60 degrees. Considering all the aforementioned results, our team estimated that the UAV takes approximately 12 seconds to perform the transition between VTOL and cruise.

Climb

The vehicle will continue to climb until it reaches the target altitude between 400 and 500 feet. Specific cruise altitude will be communicated through the FAA UTM system as certain flight levels for each drone will be required to avoid other aircraft. As the vehicle approaches the target altitude, the throttle settings will be reduced in order to level out for straight and level cruising flight.

Cruise

Between an altitude of 400 and 500 feet, the aircraft will cruise at a speed of 70 mph with each motor at a throttle setting of 45%. Control surfaces allow the aircraft to make minor adjustments to the flight path, but routes will largely be direct point to point travel.

Descent

The vehicle will begin to throttle back as it approaches the destination and is within a one mile radius. It will reduce its altitude to 100 feet and will transition back to its vertical flight configuration. Motors will be throttled back up to a 70% throttle setting to slow the descent of the vehicle to a safe speed. The aircraft has the most positional control in the vertical configuration as it is able to make position adjustments through variable thrust of individual motors. As the vehicle continues to descend it constantly scans using the detect and avoid system to ensure safe operations. As the vehicle approaches an altitude of 15 feet, the motors throttle up to hold the vehicle in a hovering flight as another checkpoint to ensure a safe landing. The vehicle then slowly descends to the ground and lands at the destination.

4.2 Energy Profile

Energy consumption, as it relates to the flight profile and endurance is an extremely important variable to satisfy the NASA requirement of completing at least one trip before being able to return to the ground center. Figure 6 shows the energy consumption profile of the UAV. The maximum power draw occurs during the takeoff phase, indicated by the steepest downward slope during that phase. This is because the motors use the most throttle during this phase of flight. The next most power intensive stage is the descent, the motors are not working as hard as during ascent, but the descent phase takes longer than the ascent phase to allow for a slow, controlled landing. The cruise phase takes the most time and consumes the most energy, however

due to the additional aerodynamic efficiency coming from the wings, this phase is actually the most efficient in terms of power draw over time.

The UAS requires less than half of it's available battery power to make one trip from the ground station, to the drop off point and back to the ground station. Unfortunately, there is an insufficient margin of safety to complete a second round trip without recharging. Alternative methods for optimizing flights to the vehicle battery are discussed in the business proposal. Due to the high velocity in cruise flight, we save enough time to replace the main battery in between trips, while still meeting the 40 minute criteria. The fact that half the charge is still remaining in the battery ensures constant performance and lower charging times. The UAS will also have an additional battery cell with the sole purpose of powering the processor and exterior sensors necessary for the collision avoidance system (CAS). If power is cut to the processor or sensors, they will need time to reboot and reintegrate their incoming data into the system, with this backup battery, we can replace the main battery pack for the motors expeditiously, without having to adjust the CAS at all. Although the main battery is not large enough to complete two 20 mile round trips, it has a safety margin of 2.1, meaning after the UAS has completed a 20 mile run, it will still have enough battery power remaining for an additional 10 miles of flight at cruise speed before dipping below 25% charge--where the voltage can be uncertain. This is important because if the aircraft were ever to drift off course or be caught in a headwind, the battery will have the longevity to ensure the mission can be completed or that the drone can be safely landed.

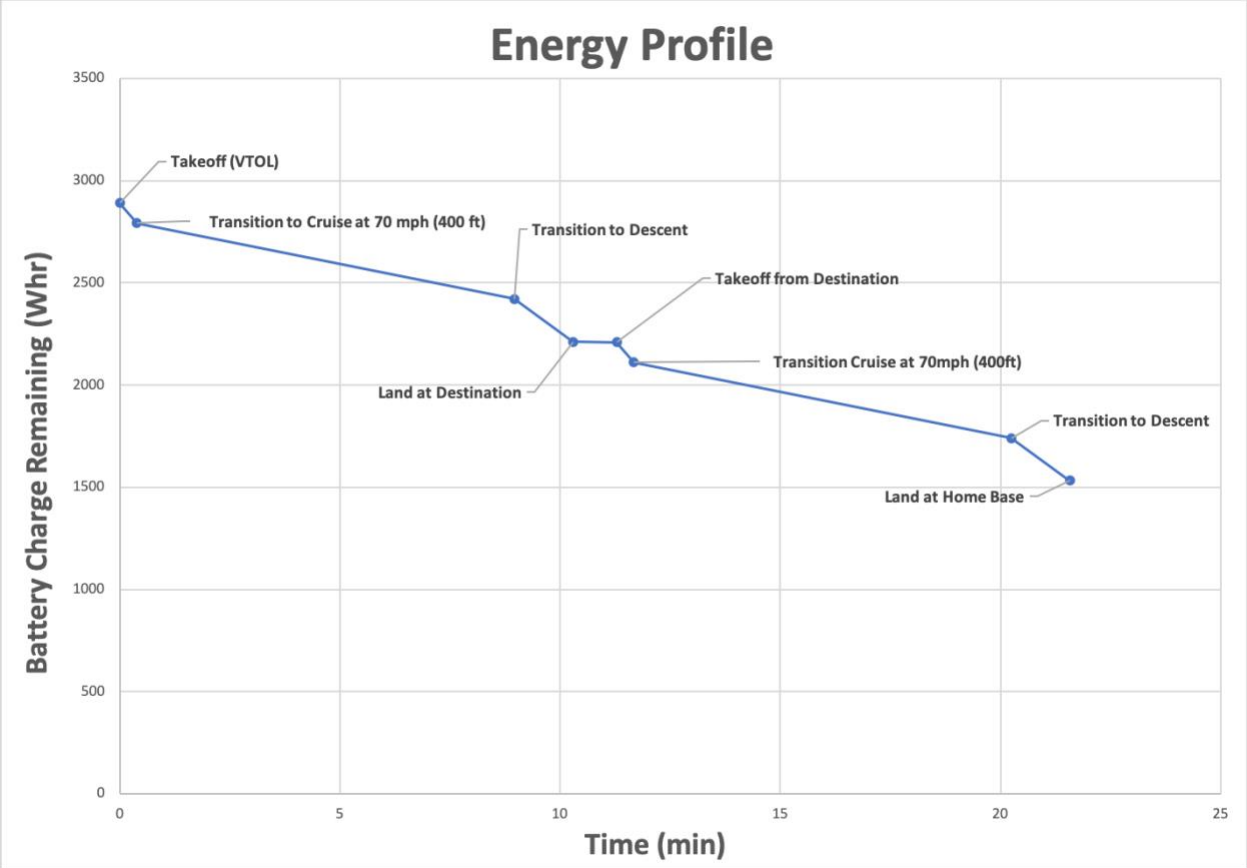

Figure 6: Energy Profile for round trip package delivery

4.3 Power System

After careful consideration and a constantly evolving selection process, the performance team settled on a lithium ion battery as the power source. The specific model is the *NCM65AH*, a commercially available battery manufactured by *CATL* (Contemporary Amperex Technology Co. Limited). Each Corvus aircraft is powered by a rechargeable module consisting of twelve NCM65AH batteries wired in parallel. Each battery costs $58, with a total of $696 in batteries for each Corvus aircraft. This configuration's mass comes out to 14.4 kg (31.75 lbm), generates 44.4 Volts, 520 maximum Amperes, and provides 2.89 kWh of energy (~200 Wh/kg of battery).

Power required is 1.36 kWh per round trip. Full specification of the batteries is provided in Figure 7.

Item		Parameter Specification
Battery Module		NCM65AH
Nominal Capacity		65Ah
Minimum Capacity		65Ah
Nominal Voltage		3.7 V
Internal Resistance		≤0.5mΩ
Charging(CC-CV)	Maximum Charging Current	130A
	Charging Upper Limit Voltage	4.25V
Discharging	Maximum Discharging Current	520A
	Discharging Cut-off Voltage	2.8V
Charging Time	Standard Charging	1h
	Quick-acting Charging	0.5h
Recommended SOC Usage Windom		SOC: 10%~90%
Operation Thermal Ambient	Charging	-5°C ~ 55°C
	Discharging	-30°C ~ 55°C
Storage Thermal Ambient	Short-term (within 1 month)	-20°C ~ 45°C
	Long term (within 1 year)	-20°C ~ 25°C
Storage Humidity		< 70%
Battery Weight		1,200±25g
Battery Dimension		148 x 130 x 27 mm
Shell Material		Aluminium

Figure 7: Battery Specifications for the CATL NCM65AH

4.4 Power Supply Selection Process

In determining a suitable power supply for the aircraft, a set of primary and secondary goals were established. Throughout the length of the design process, the team constantly found itself re-prioritizing secondary goals, while the primary goals remained the same.

Primary Goals

1. Meet the minimum energy requirements for the craft. This includes all propulsion systems, as well as sensor arrays, computer systems, servos, and any other systems that require power.

2. Provide a safe and reliable power source.
3. Find a power source that does not inherently contribute to increased aircraft noise.

Secondary Goals

1. Minimize energy costs. Several decisions that factor into this include the cost of the hardware, the cost to recharge/refuel the hardware, and the expected lifespan and maintenance costs of the hardware.
2. Provide a source of high energy density in order to reduce the mass of the power source (and in turn, reduce craft weight).
3. Employing hardware that lends itself to being recharged/refueled easily and quickly in order to minimize aircraft downtime.
4. Compact hardware that can easily be compartmentalized and concentrated within the body of the aircraft.

Even before a design was established, the team's earliest meetings ruled out traditional fuel cells. Fossil fuels violate two of the primary goals. Even if a suitable, efficient combustion engine *could* fit on such a small craft, the noise and air pollution are unavoidable. More importantly, the combustible fuel creates an unsafe, low-flying hazard in urban airspace. Given these drawbacks, the team unanimously agreed on electric batteries.

Unfortunately, batteries are not known for their high energy density. The most cutting-edge lithium ion batteries can barely reach 300 Wh/kg (Watt-hours of energy per kilogram of battery) while standard petrol averages around 12 kWh/kg of fuel. This became an issue in the first round of preliminary metrics. Based on numbers provided by both aerodynamics and propulsion teams, an incredibly high energy consumption of ~11kWh was estimated. Even with

experimental 300+ Wh/kg lithium ion batteries, this would have required 36.7 kg (80.9 lbf) of battery packs in order to simply meet energy requirements.

During this time, alternative and experimental batteries were sought out, many of which had yet to even reach production. This investigation led to a small startup in Cambridge called *SolidEnergy Systems*. Their solid state *Hermes* battery technology was already available for purchase, and its technical aspects were superior in nearly every way to all commercially available batteries. The energy density nearly doubles lithium-ion and lithium polymer batteries. In addition, research papers claimed that solid state batteries recharged faster and held greater lifespans. When it came to safety, the solid state technology also trumped other batteries - it replaced liquid, organic compounds with solid electrolytes that reduced heat generation by nearly 80% and nearly eliminated flammability.

With the ability to meet power quota with less than half the initial battery weight estimate, the *SolidEnergy* Hermes battery emerged as the frontrunner. Unfortunately, the cost per battery turned out to be a huge drawback, as each 186 gram battery pack cost $300 USD.

As design iterations became more refined, propulsion and performance teams continuously re-evaluated energy requirements. Within two months of the initial 1l kWh figure, newer data suggested that the craft required ~5.1 kWh. The steep price of the solid state batteries gave rise to concern. While the energy density was certainly higher, the price per kWh was significantly higher than commercially available competitors. Figure 8 shows a comparison of these prices.

Battery	Wh/kg	Mass/battery	Price / Battery	Projected Mass (kg / lbm)	Projected Price
SolidEnergy - Solid State	450	0.186 kg	$300 at 0.186kg	11.34 / 25	$18,000
CATL 50 AH - Lithium Ion	205	0.9 kg	$40 @ 0.9kg	24.89 / 54.87	$2,440
Catl 120 AH LiFePo	137	2.8 kg	$60 @ 2.8kg	38.24 / 84.33	$840
Projected Energy Req: 5103 Wh					

Figure 8: Comparison of Battery Masses and Prices at 5103 Whr required

The power consumption numbers in this report indicate that the final energy numbers were determined to be far less than even this checkpoint estimate. With the much lower requirements, cost became a much greater concern. At this point, the significantly better energy per cost ratio became much more attractive. Furthermore, specific lithium ion batteries with high current tolerances allowed the propulsion team to wire each motor individually in parallel circuits. This allowed for greater control and redundancy in case of individual motor failure - a problematic circumstance for motors in any combination that included series circuitry.

As for the specific battery itself, the NCM65AH found itself the best fit within the aforementioned criteria. Around one in four electric vehicles runs on a CATL battery, with companies such as Honda, Toyota, Volvo, and most recently Tesla trusting their hardware. A set of 12 parallel-wired NCM65AH packs meets the voltage and current requirements while generating twice as much energy as the required trip demands. The dimensions of each individual pack also makes for a convenient fit within the aircraft's interior, allowing for a compact module housing all the batteries in one location. The final tipping point came in the form of cost - with a bulk order, each pack comes out to $58 USD. This allows the drone manufacturer to pay just under $700 for each delivery craft's power source.

5. Propulsion Summary

5.1 Motors

The propulsion system on the aircraft features eight MAD M10 IPE 150KV motors; two on each wing located at the wingtip and at one third semispan, respectively, with variable pitch MAD 22” propellers and 80A ESCs. This decision was motivated by a variety of factors including thrust requirements, redundancy, power constraints, wing size constraints, and noise production limitations.

First, the decision was made to use electric motors for propulsion. Other considerations were made, such as reciprocating or turbine engines, but ultimately neither proved to be a viable competitor. The primary draw of a power plant independent of battery power was the energy density of the hydrocarbon fuels they use, which can be up to 100 times greater than modern lithium batteries (Gur et. al, 2009). This would have resulted in an effectively unlimited range for the aircraft. Unfortunately, this benefit is negated by the losses in efficiency when these power plants are scaled down to sizes which could be used in a drone and the difference in noise production between electric and traditionally fueled power plants. Scaled down turbines and reciprocating engines are significantly less efficient than their full sized counterparts, requiring them to be larger and heavier than an electric motor capable of producing similar amounts of power (Gur et. al, 2009). They also have significant changes in power output and efficiency depending on operating speed and throttle. In contrast, electric motors have an almost entirely linear power curve and almost constant torque, making them much more efficient and predictable, especially at low throttle settings (Ryan, 2016). Even with these weight and efficiency limitations jet turbines could still have been viable alternatives if not for their noise production. The extremely high speed air flow required to produce thrust in a turbine results in

noise production that is unacceptable in a low altitude urban environment. In contrast, electric motors produce minimal noise, significantly less than that which will be produced by the propellers they are paired with. While research is being performed on minimizing turbine noise it is not yet sufficient to be a viable choice.

Next, the craft required sufficient excess thrust to climb and cruise at acceptable rates. Initial sizing estimates placed the weight of the aircraft between 100 and 150 pounds, and a minimum thrust to weight ratio was set at 1.5 in order to provide enough excess thrust for acceleration and control during vertical takeoff and transition to cruise flight. This number was motivated by the climb requirements of the challenge and the testimony of experienced drone pilots, who state that 1.5 is the minimum thrust to weight ratio to effectively control a drone during takeoff (Drone Omega, n.d.). The MAD M10 produces a maximum static thrust of 24.25 pounds when paired with the 22”x10” propeller, as stated in the company’s technical specifications, resulting in a maximum thrust of 194 pounds of static thrust (Mad Components, 2020). The final weight of the aircraft came out to be 103 pounds, resulting in a maximum thrust to weight ratio of almost 2. However, due to the power curve on electric motors no losses occur as a result of decreasing the throttle. The only losses come from unnecessary motor weight, but it was decided that 1-2 pounds of excess motor weight is an acceptable price for an additional 0.5 thrust to weight ratio that could be used in emergencies.

Finally, we elected to use variable pitch propellers in order to maximize efficiency in both cruise and takeoff, at the cost of some added weight and complexity. Initial results of MotoCalc simulations found that no fixed propellers could perform efficiently at both static and cruise conditions. High pitch propellers would stall in static conditions, resulting in loss of thrust and low pitch propellers did not have sufficient pitch speed to provide thrust while cruising at the

maximum velocity. As such, a variable pitch propeller was deemed necessary to allow the aircraft to function in all regimes.

5.2 Motor Arrangement

An eight motor design was selected to propel the aircraft. This decision was motivated by a variety of factors, but primarily the desire for redundancy in the propulsion system and the constraints of the aircraft's wing size.

In the event a motor fails during vertical flight the aircraft must disable another propeller on the opposite side to maintain control. This reduces the amount of lift available and, more importantly in some motor configurations, can reduce the number of control axes on the aircraft. We determined that, in order to maintain both lift and control, the minimum number of motors on the aircraft would have to be 8. Any fewer than this would result in either loss of an axis of control in configurations with fewer than six motors or a loss in lift that would take the aircraft to a lift to weight ratio of 1 or less, meaning the mission could no longer be achieved.

More than eight motors would have provided greater redundancy for the aircraft, but at the cost of propulsive efficiency due to wing space requirements. Given the decision to mount motors to the front of the wings it is only possible to have propellers with diameters adding up to the wingspan of the aircraft plus one extra propeller radius extending beyond the wingtip on either side. Ideally, the propellers would be as large in diameter as possible, as larger propellers are more efficient than smaller propellers and produce more thrust than multiple smaller propellers that sum to the same diameter. As such, it was determined that an ideal configuration would have two propellers on each of the four wings, each with a propeller diameter of approximately 1.5 times the aircraft's semispan. In the final configuration these propellers would be reduced slightly to 22 inches in order to reduce weight and the torque required from each

motor, as they were found to produce sufficient thrust. That did not, however, result in sufficient excess space for a third motor on each wing.

5.3 Noise Assessment

Serious commercial drones produce a lot of noise as they have eight or more propellers at thousands of revolutions per minute, physically beating the air to generate lift and movement. The heavier the load, the harder they have to work, the more air gets beaten – and the louder the sound. This sound is also amplified with hundreds of other drones delivering packages to homes and businesses. Therefore, it is important to understand possible unique aspects of annoyance due to noise from these vehicles. The key question is: At what distance will the UAV's noise propagate? It is important to note that the size and aerodynamic characteristics of the UAVs in particular make their flight path susceptible to atmospheric disturbances such as wind gusts. These gusts, combined with our drone's flight control system which varies rotor speed to maintain vehicle stability, creates an unsteady acoustic signature. This may affect how much sound is registered by the ear.

To reduce our predicted noise signature, we used electric motors with propellers instead of the far noisier jet engine options. We used two bladed propellers, which disturb the air less, and preferred larger diameter propellers, which can be spun slower to further reduce the noise signature. The choice of only eight motors also reduced the noise profile over more propellers. Though even fewer propellers would have made our noise more tolerable, for safety and redundancy we needed to have at least 8. Our rough calculations show our drone producing 81 dB of sound when 2 meters away from a person. While high, it is important to note that this will be a small fraction of the flight, only during landing. Sound intensity falls as the distance squared, so at our cruising altitude of 400 ft, the drone will be very quiet. Constructive

interference of multiple drone sounds could be an issue, though traffic management will likely try to keep drones far apart to prevent crashes, which will also reduce noise.

6. Infrastructure Summary

6.1 Ground Systems

The ground systems facility for the drones will allow the vehicles to be loaded and recharged completely autonomously for as many trips as necessary. The main benefit of this system is that it allows for the quick turnover of multiple drones for package delivery trips as required by our business plan. The overall structure of this system is presented as follows.

Step 1: Initial Landing and Damage Identification

Upon returning from a package delivery trip, the drones will land on a designated platform. An inspector will look over the vehicle to assess any damage it may have sustained. If damage is found, the vehicle will be taken to a seperate area for repairs. Otherwise, a conveyor belt within the platform will move the UAV onto the main assembly conveyor belt. This automated mechanism will move the drone into the packaging and recharging assembly.

Step 2: Packaging and Battery Replacement Assembly

In this stage the packaging and battery replacement will occur in three steps and is depicted in Figure 9. First, the drone will open its bottom bay doors and an automated platform (**A**) will be raised into the drone just below the battery pack. Next, the drone will release the push-activated latching mechanism (PALM) holding the battery pack in place thereby releasing it onto the platform (**B**). This mechanism is similar to the latching mechanism used to hold car hoods in place. The platform will lower itself, and the used battery pack will be taken away for

recharging using another conveyer belt (**C**). Next, the drone will be moved further down the assembly line where a new, fully charged battery pack will be lifted into the drone using another platform (**D**). The PALM system will hold this new battery pack in place for the duration of its mission. Finally, further along the assembly line a platform will place its designated package into the drone. This package will be held in place using a smaller version of the PALM system inside the battery pack.

Step 3: Exit and take-off

At this point, the drone will be fully charged and have its next package for delivery. The drone will continue down the assembly line and exit the distribution center on a final platform. From here it will receive its delivery destination and will take-off to complete its mission.

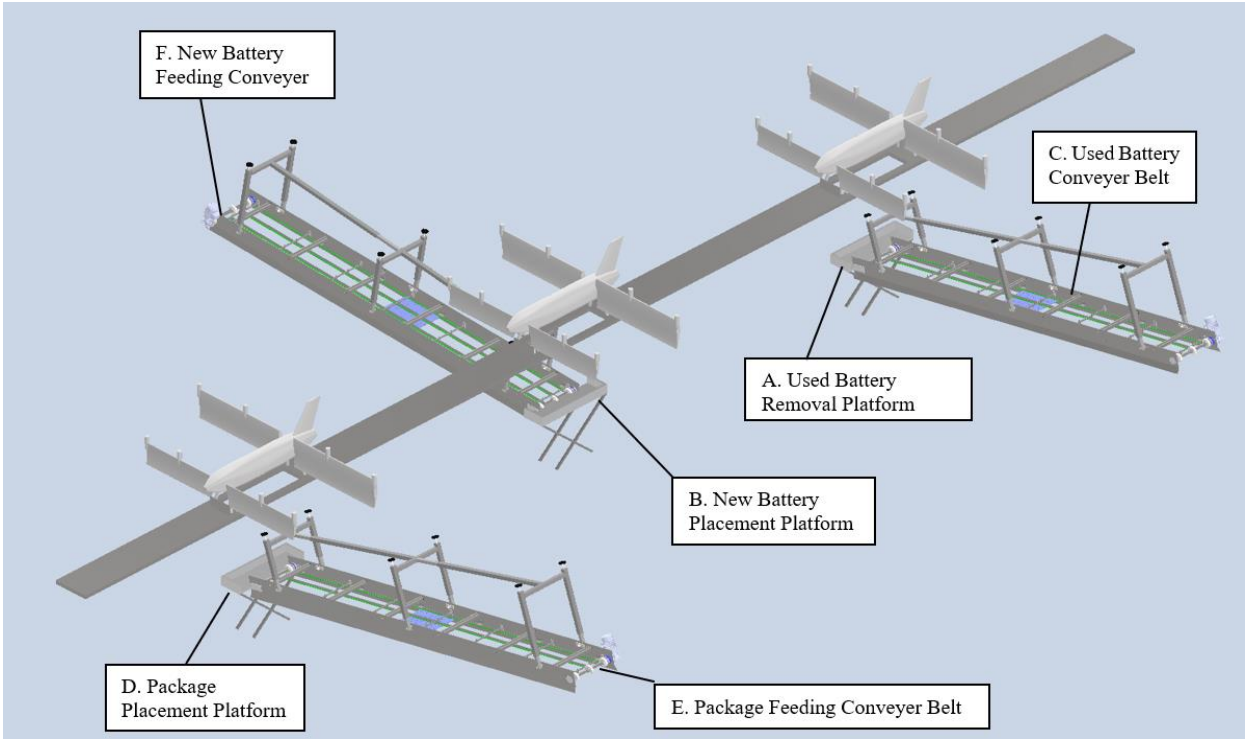

Figure 9: Drone Packaging and Battery Replacement Model (Parts F, C, and D created by Safarabadi)

6.2 Autonomous Handling Architecture

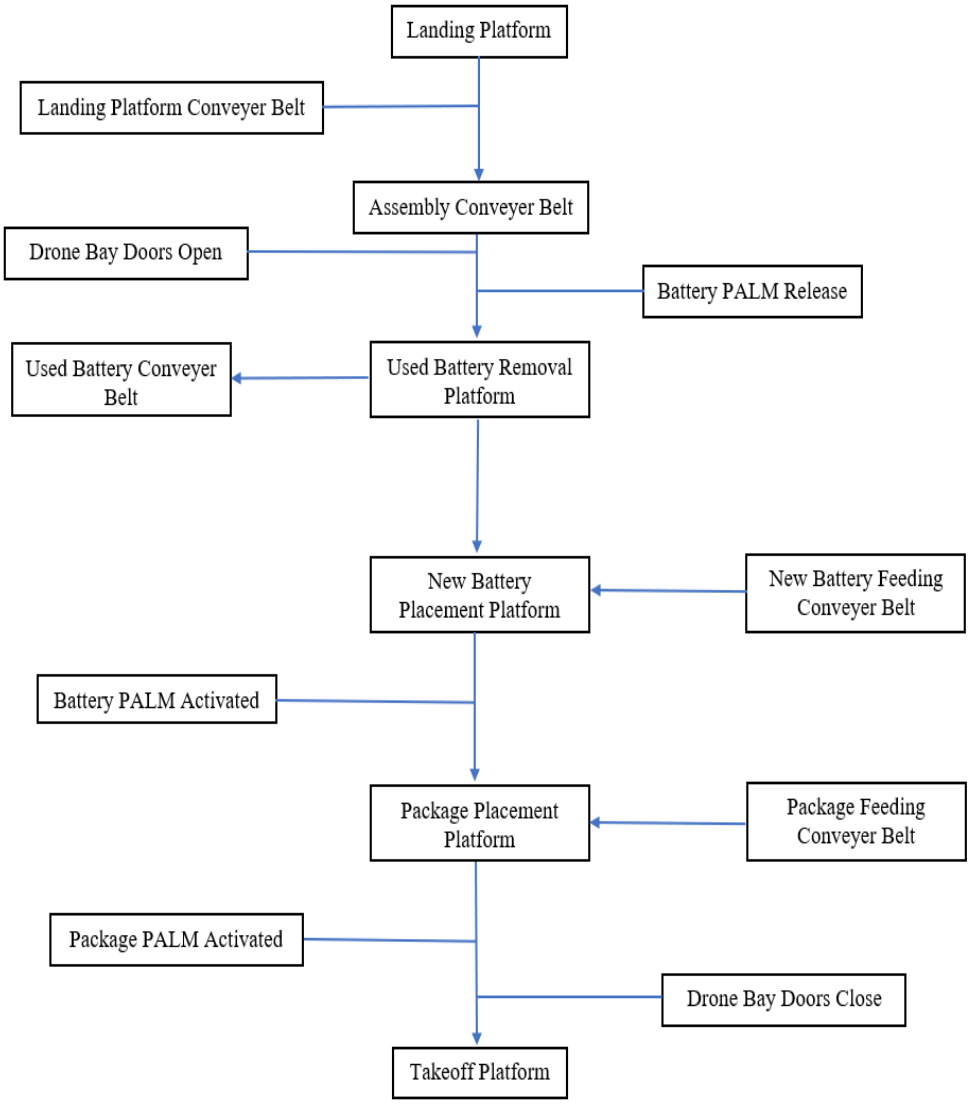

Figure 10: Autonomous handling schematic

7. Cost/Business report

7.1 Vehicle Costs

Table 6 summarizes the cost breakdown of a single UAV. We assume that under bulk purchasing deals we could save 25% off of the component costs. This is reflected in the final price per drone of $10,033.

Table 6: Cost breakdown per-drone

Vehicle component	**Item Cost**	**Total Cost**
Propulsion System	-	**$3,896**
Motors	$2,136	-
ESCs	$800	-
Propellers	$960	-
Computers, Sensors, etc	-	**$4,110**
Batteries	$660	-
Cameras	$900	-
GPU	$500	-
Computing and IMU	$1,850	-
Sonar	$200	-
Structure, Safety	-	**$8,550**
Airframe Foam	$200	-
Airframe Carbon	$600	-
Airframe Aluminum	$250	-
Control Surfaces	$1,300	-
Servos	$200	-

Parachutes	$6,000	-
25% bulk purchase discount	$16,556	**$12,417**
In house manufacture of parachutes, computers, etc	-	**$10,033**

Overall, for the assumed single facility fleet size of 30 drones, the total vehicle cost amounts to $372,510. The initial prices represented above all are from off-the-shelf components, which would make present production of a prototype Corvus drone possible. However, the off-the-shelf pricing does lead to a higher initial cost of $16,556.This cost is trimmed down by assuming a bulk discount of 25%, which would represent the manufacturing and supplying contracts made. This number would obviously not be standard for all components and suppliers, but represents an average for all parts. In house product development can also lead to vast product cost reductions. This is especially true for the parachutes, sensors, and propulsion systems. Part cost reductions of roughly 50% can be obtained by reverse engineering these components and systems (Drummond and Yang, n.d.), improving upon the 25% reduction from bulk purchasing. This leads to a revised final price per drone of $10,033, assuming in-house development of the entire propulsion system, sensors, IMU computing, and parachutes. Manufacturing cost of a single Corvus drone is included in the 50% of the components that will be made in-house. This also includes the final assembly of all components into a single vehicle.

Development costs also comprise a significant component of drone program cost. The development cost for the drone program is estimated at $2,838,000. It is summarized in the table below. Cost models come from Willcox, 2004.

Table 7: Development cost of Corvus Drone Program

Development Cost				
	$/lb (2004)	$/lb (2020)	Weight (lb)	**Total Cost ($)**
Wings/Tilting	69,887	95494	14.2	1,356,015
Fuselage	52,156	71266	9.3	662,774
Propulsion	8,691	11875	14.1	167,438
DAA/UTM/ Software	34,307	46877	13.76	645,028
Payload System	10,763	14707	0.5	7,354
Total				**$2,838,607**

7.2 Facility Costs

The cost for an average distribution center is estimated to be $6 Million. This figure is derived from both average warehouse costs per square foot and from construction costs for Amazon fulfillment centers. Also, this takes into account the retrofitting of existing logistics centers already in urban areas, which would require only small modifications.

New fulfillment centers would come in at approximately $25 million (BDC Network, n.d.), and retrofitted warehouses would cost only $1 Million (Keeney, 2015) Estimating that a new distribution center with drone infrastructure would occupy 400,000 square feet and with warehouse costs estimated at and average of $20 per square foot (BuildingsGuide, n.d.) results in an $8 Million price tag. However, this figure does not include storage and package movement infrastructure, which is estimated to cost around $4 Million. This figure derives from the cost for a Small Package Sorting System machine (USPS, n.d.), which handles mail for the US Postal

Service. This size of square footage was chosen as it represents the lower end of Amazon's distribution center size. Space limitations would make warehouses that occupied more space prohibitively expensive and impactful in dense urban environments. Additionally, analyzing the costs for Amazon's distribution centers, smaller fulfillment centers would cost around $25 Million, when downsizing from larger, new centers. New distribution centers would have to be large enough to carry many items, however, as they are going to be primarily drone based, they would not need to allocate storage and operational space to the shipping of large and heavy items that would not fit inside of the drones.

The cost to retrofit existing fulfillment centers with a station for drone shipping is estimated to cost $1 Million (Keeney, 2015). Only small modifications would be necessary to logistics centers to add in the necessary loading infrastructure for the drones. This would require a section of the warehouse to house spare drones, batteries, and parts, and maintenance equipment. Additionally, package movement infrastructure, represented either by conveyor belts or drone systems, would need to have their structures and software modified to send packages individually and quickly to the drone loading station. Also, cordoning off a section of ground pavement to be used for the installation of takeoff and landing platform infrastructure is necessary. Local UTM communication infrastructure costs are unknown, but are estimated to be less than $250,000 per fulfillment center. As many large fulfillment centers are already located around major metropoles, a majority of package drone accommodations would take place through modifying existing warehouses instead of building new ones, the average cost is $6 Million.

7.3 Operating Costs

The operating costs refer to recurring costs that package drone delivery systems incur. These include staff salaries, drone parts, battery electricity, operating licenses, and insurance. Table 8 summarizes the costs, and the remainder of this section provides justification. Labor represents a large component of operating costs, as the exact number of dedicated drone employees is unknown. Depending on FAA regulations regarding the number of operators allowed per drone, staffing costs can fluctuate greatly. One study suggested that a single dedicated drone controller would be able to oversee around 10-12 drones, which contributed to a per-package cost of under $1 (Keeney, 2015). A separate study assumed that each drone would require two exclusive operators, contributing to a package cost of $17.44 (Robot Economics, n.d.). The average pilot's salary was estimated to be at $50k annually by both studies. This demonstrates the dependency of this venture's profitability on the changes to FAA regulations, which will be discussed shortly. Assuming each facility would have around 30 drones in the air at any given time (Sudbury & Hutchinson, n.d.), this would require between 3 and 60 operators, causing pilot labor costs to range between $150k and $3M annually. An estimate of one operator per drone will be used as a compromise, giving an annual pilot cost of $1.5 Million, though it is highly likely that this value will be far lower given ideal FAA regulation changes. Additional staffing costs that are unique to drones at fulfillment centers are drone mechanics. Each mechanic makes on average $42,000 each year (Indeed, n.d.), and assuming that six mechanics will be full time employees to provide around-the-clock service, maintenance staff accounts for ~$250k annually. Other increases to labor costs, such as those of cleaning, parcel machine repair, and administrative staff will add on an estimated $200k annually.

Drone parts represent the largest expense to operation, specifically batteries and motors that will wear out over time. As mentioned earlier, each drone requires 12 individual battery cells, resulting in a battery cost per drone of $660. Motors cost $2136 per drone. The cost for spare parts can be equated to roughly 1/7th the cost of a single drone (Keeney, 2015). Therefore, an estimate of $1,450 will be spent on having spare parts. According to one study, maintenance comprises roughly $4,000 for a single drone over a five year lifespan (Sudbury & Hutchinson, n.d.). However, these are based on a lower initial drone price of $5,000, rather than our $10,000. This increases the five year maintenance cost for a drone to $8,000, giving it an annual price of $1,600.

Electricity and charging also represent a significant cost to operation. Each drone has a total of approximately 3 kWh in its batteries, and assuming a cost of electricity of around 8.5 cents/kWh (Commercial and Industrial) (EIA, n.d.), a full journey would cost just over 25 cents. And assuming each drone completes 25 full journeys every day (which results in 750 total daily deliveries), each drone will cost $6.25 in power daily, extrapolated to ~$225k annually. Licensing and insurance costs are still key aspects to consider in terms of pricing, but on the whole they do not constitute significant charges relative to labor, parts, maintenance, and electricity.

Table 8: Operating costs per drone, per year

Component	**Cost**
Annual pilot cost (1 per drone)	$50,000
Annual Mechanic cost	$8,400
Annual Support Employees	$6,666

Annual Maintenance cost (parts)	$1,433
Annual Electricity ($.085/kWh)	$225,000
Total	**$291,500**
Total for drone fleet (30 drones)	**$8,744,978**

7.4 Regulatory Issues

The development and operation of a profitable drone delivery service requires the approval of the Federal Aviation Administration (FAA), which, to date, has been a sticking point for getting started. Current FAA regulations do not permit the autonomous operation of any drone, or the piloting of a drone outside of visual line of sight (FAA, 2019). Additional pertinent restrictions for the UVA drone include: drones cannot fly at night, drones cannot fly over people, and drones cannot fly over 400 ft above ground level (FAA, 2019). The FAA has shown willingness to waive the latter restrictions if a convincing argument is made by the applicant, and rules like flying at night have an 86% approval rate (FAA, 2019). However, to date, no applicant has successfully argued for autonomous flying, which is something this drone operates with. If this team gains approval for fully autonomous operation, then any costs associated with pilots will be moot. The best case study for gaining large FAA approval is UPS Flight Forward Inc, which was the first, and only, operator to receive the highest part 135 certification for package delivery (Dronelife, 2019). That approval grants everything except autonomous operation. Wing, another operator, received more limited approval earlier, so they can be used as an example too (Dronelife, 2019). All told, the issues with FAA certification mean that "companies like Amazon.com have increasingly moved their UAV operations overseas." (ProfitableVenture, n.d.)

To operate the Corvus, companies would need to take advantage of overseas markets while simultaneously pushing for FAA certification at the highest part 135 level with another waiver for autonomous flight. It is unknown how UPS structured their application to win the first approval, as the application is not public, but the FAA does provide a minimum list of requirements that an operator would be required to meet. The operator must own the aircraft, have a specified director of operations, chief pilot, and director of maintenance. In addition, the operator must conduct inspections and maintenance every 100 hours of flight time, and detailed annual inspections (FAA, 2020). Also, general, maintenance, and flight manuals are required for the craft (FAA, 2020).

In a deal to sell the Corvus to a company, the team would sell the additional products and services to achieve regulatory compliance. A full maintenance plan with detailed annual and 100 hour inspection procedures would be sold in addition to all the pertinent manuals. The drone would also be rigorously tested with FAA supervision to achieve autonomous certification before it would be put on the market. The UVA UAV team would also provide training to the purchasing organization on how to operate the drone, contingency procedures, and achieving approval from the FAA.

7.5 Competing Enterprises and Profitability Model

Our drone is able to fulfill the requirements for delivery time and distance as stated in the NASA competition requirements. Given the amount of drones present in a facility being 30, one drone can take off every 2 minutes for an hour easily, even without factoring in drones returning to the hub. Additionally, as mentioned above in the Energy Profile section, our drone is capable of doing a 20-mile round trip journey to deliver a package. However, the UVA UAV team has designed the Corvus to go above and beyond this initial requirement, emphasizing speed and

range. As a result, a single drone is capable of delivering a package out to a distance of 15 miles from the distribution center, for a 30 mile round trip. This increases each logistics center's delivery area from Just over 314 mi^2 to over 700 mi^2, enabling an increase of serviceable destinations by 125% (assuming homogeneous population density). This greatly increases the effectiveness of each distribution hub. Also, given the power capacity of each drone, multiple shorter trips on a single charge would be possible as well. For example, one drone would be able to perform two 7-mile deliveries on a single charge. This keeps each drone flying for longer and reduces the number of batteries and charging stations that need to be purchased.

The Corvus is also able to provide extremely rapid delivery for a single package, even at far distances from the distribution hub. Given the 70 mph cruising speed of the Corvus, it takes just under 15 minutes of travel time to reach a destination that is 15 miles away (factoring in slower speeds during climb and descent). Assuming a package fulfillment time of ~15 minutes from receiving the order to having it ready to ship, this can offer 30 minute delivery times to an entire city.

Both of these accomplishments are impressive, but the most attractive part of the Corvus's business model is its very inexpensive delivery charge, charging only $4. Many projections exist regarding how much it should cost for a single package to be delivered by drone, but none fit the exact case of the Corvus. Existing predictions assume that operator costs are far lower or far higher than ours, or use less expensive drones (Keeney, 2015; Jenkins et al., 2017; Robot Economics, n.d., Sudbury & Hutchinson, n.d.). As a result, a midpoint of these was established. The cheapest delivery fare was at $1 per package, while the worst was at $17. All projections had individual drone costs between $2000 and $4000. Most also assumed that multiple drones could be controlled per operator. As the Corvus is more expensive than these

cheap drones, it will not be able to provide service at the low $1 charge. However, extrapolating from the inexpensive cases and factoring in higher pilot and capital costs, the price of $3.86 was obtained. This enables packages to be shipped for $4, or for less with a subscription. However, this price will quickly drop given the increase in number of autonomous drones given to each pilot to monitor. Seen in Figure 11 below is a comparison among current shipping options. A 30 minute delivery for a $4 charge still improves upon all existing shipping methods, both in cost and delivery time. FAA permission for fully autonomous flight would essentially remove this charge.

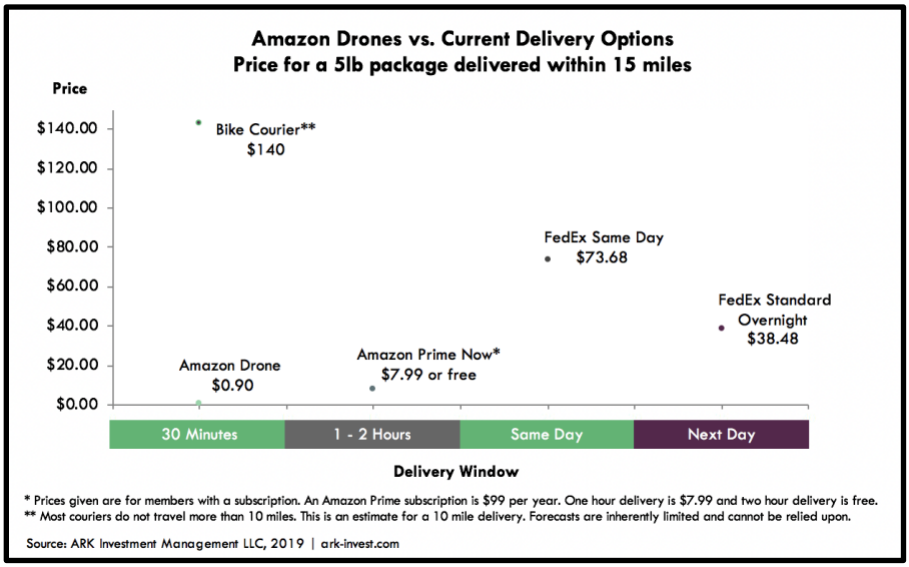

Figure 11: Pricing of various modern shipping methods (ARK-Invest, 2015)

The need for drone delivery also represents a massive, untapped market. Projections suggest that drone delivery will be a $63.6 Billion industry by 2025 (Business Insider, n.d.). Additionally, the package weight required for this competition, 5 pounds, constitutes 86% of all packaged delivered by Amazon, according to Jeff Bezos (Keeney, 2015). With Amazon's

shipping costs increasing annually (Statista, n.d.), the sooner systemic savings can be implemented, the better. Moreover, it is estimated that up to 25% of the destinations of these packages will lie within 10 miles of an Amazon distribution center (Keeney, 2015), which can be expanded to 35% for a 15 mile radius. While some of these packages would not be small enough to fit into the 6x6x6 inch package required for this competition, a significant portion of these items would still fit this threshold. Using drones instead of vans or trucks to deliver these parcels would result in massive financial savings. One article proposed that if every UPS delivery van travelled one fewer mile each day, that would amount to $54 million in fuel cost savings (Fleet Owner, 2018). Extrapolating this to the thousands of miles that one hub's drones would cover in a single day, this would save companies billions. An additional benefit of replacing polluting delivery trucks in urban areas with electric drones would be an improvement in air quality. Postal and delivery vehicles also stop frequently, contributing to road congestion, which would be improved through the deployment of package drones.

The Corvus also demonstrates a high degree of safety. Each drone features many redundant safety features and has failsafes. The use of 8 motors can still enable the Corvus to fly should an engine fail. The motors are also powerful enough to help the Corvus safely land in the event of system failures or poor weather. Failsafe recovery parachutes also prevent the possibility of the drone falling out of the sky at speed. Many sensors also aid in having safer landings, as the Corvus will not land if it means endangering people. For public security, all footage of people that may be recorded during landings is swiftly deleted. These features all help to demonstrate commitment to safety and security, which were rated as imperative to drone delivery consumers in one study (NASA, 2018).

8. Safety

8.1 Detect and Avoid

The proposed drone design utilizes a Detect and Avoid (DAA) system for autonomous guidance, navigation, and controls. The DAA system is primarily driven through a real-time application of neural networks run on a central processor, receiving data from an array of sensors installed on the drone. The sensor array includes a sonar sensor and stereo cameras.

The sensor array has these particular sensors to ensure that the drone will be able to operate across a wide variety of expected and unexpected hazardous conditions. The variety in the types of sensor used ensures that the DAA system is more reliable and adaptable from utilization of multiple signal domains (ultrasonic, visual), ensuring a continuity operation when encountering adverse situations when one or more signal domains are compromised or unavailable. Another rationality in usage of multiple signal domains, is that each domain possesses different strengths in certain conditions and situations. With an ultrasonic sonar sensor, the drone gains an adaptable sensor that can operate in most adverse conditions as it is not affected by any particles in the air such as atmospheric dust, rain, or snow. Furthermore, ultrasonic sonars have the ability to detect all material types with good range capabilities. However, the downside with the ultrasonic sonar is that it is sensitive to the changes in temperature of the atmosphere since it uses sound wave propagation. Also, it has a hard time detecting objects with certain properties. Objects with narrow profiles with respect to the field of view of the sonar, as well as soft, and curved objects create detection issues. These weaknesses are covered by the stereo camera. While stereo cameras can be limited in range visibility from rain and snow since it relies on unobstructed vision, it does not suffer from the weaknesses of

sonar. While sonar would have trouble with thin or soft objects such as electric lines or home antennas, it would have no problems in detection with a stereo camera. (Sonar System, 2014).

In the proposed navigation system, the detect and avoid sensors feed their data into a neural network capable of object detection. Through this capability, the computer ensures that the drone is able to navigate amongst any set of obstacles presented during delivery. To achieve such adaptability, the neural network requires extensive testing and "training" on data to ensure that it has learned enough about a typical terrain encountered during delivery. The primary focus of the training data set for the neural network is for near ground VTOL flight. This is because the greatest amount of variability in situations occurs near the ground where the highest probability of object collision occurs since it is the zone with the highest number of objects within the drone's trajectory. The primary objective of adaptive learning is to achieve a safe and reliable package delivery through any presented situations. The proposed training method is a supervised learning method, where the parameters and variables that the drone will learn from are predetermined. This is to ensure that the training on the data set is fast.

During non-VTOL transit part of the delivery, the majority of the controls are handed off to the Piccolo flight controller, which mostly handles controls, as well as handling route handling and FAA UTM regulation compliance.

8.2 FAA Airspace Integration

NASA Ames Research Center and the Federal Aviation Administration are working towards an Unmanned Aircraft System Traffic Management (UTM) system. The drone designed for this project would ideally be incorporated into this system as this technology begins to be implemented across the country. The vision for this UTM system is to allow operations of drones that are beyond a visual line-of-sight while managing the airspace in a safe manner. The figure

below shows the possible components of the UTM system and how they would work together to create safe operating conditions.

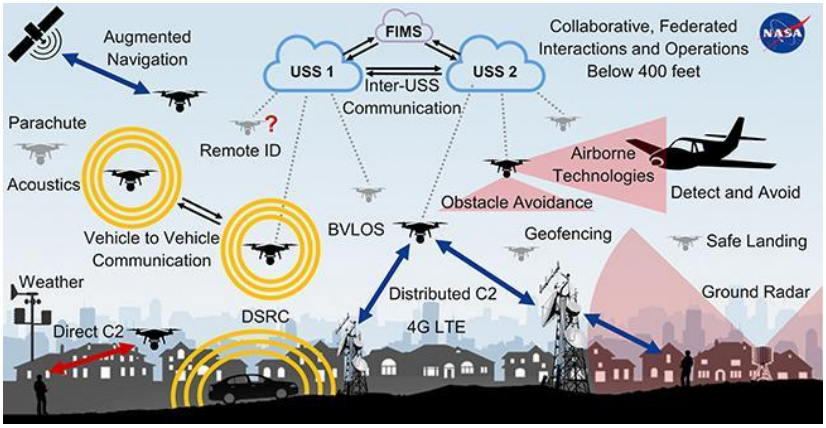

Figure 12: NASA UTM Concept (Rios & Boyle, 2020)

Current FAA regulations include certain requirements that would not allow for the operations outlined in this challenge. These include weight requirements of under 55 lbs, operation in class G airspace only, remaining in the pilot's line of sight, and never flying over groups of people/heavily populated areas. While we recognize the existence of these regulations, we believe the development of the UTM system and advances in autonomous flight will allow for operations similar to those we outline.

8.3 Redundancy

Per NASA requirements, our drone has to be safe and reliable. To this extent, our drone is fitted with redundancy measures through our motor configuration, control surfaces, independent motor control, and computer architecture. In the event of partial system failure, our redundancy system in our drone is able to prevent performance decline from exceeding specification limits without the need for human intervention.

Having eight motors is an inherently redundant system. In our implementation, these motors also employ an active redundancy system through voting logic. Active redundancy eliminates a decline in performance by monitoring the performance of individual devices. Here, this monitoring takes the form of voting logic. In voting logic, performance is monitored in order to determine how to reconfigure individual components so that operation continues without violating limits specified within the overall system. This means that in the event that one or more propulsors fail, the other propulsors would increase or decrease their performance accordingly. In addition to an active redundancy system, the vertical fin acts as a passive redundancy system. For example, if one of the side propulsors fails, the vertical stabilizer is large enough to counteract the induced yaw.

Additional redundancy systems include the use of its nine servos (see Appendix G). The back wing is equipped with a DA 30 high torque, front wing with a DA 30, and smaller servos for the side motors and smaller control surfaces. If one control surface fails to operate due to a servo failure, the drone is still able to be controlled through the use of other servos and control surfaces. Taking the worst-case scenario as an example, if a servo controlling a wing fails, the drone is able to maneuver itself using its various other smaller control surfaces.

The computer architecture is also an active redundancy system. The flight control processor has internal sensors which share their data to the detect and avoid system, and both systems can output commands to the motors, control surfaces, and servos to safely guide and navigate the system. Therefore, if one fails the other can launch a contingency or emergency landing. In addition, the detect and avoid system is equipped with multiple ultrasonic sensors and stereo cameras. If one of these sensors fail, the drone is still able to perform detect and avoid maneuvers with the remaining sensors.

On top of all this, the drone has a 2.1 safety factor in its battery life and 1.5 safety factor in structural rigidity. Our drone's battery enables it to complete the prescribed mission with 2.1 safety margin which allows for any emergency maneuver or to meet a mandatory increase in performance. Structural elements were also designed with a safety factor of at least 1.5, since structural failure is a very dangerous failure mode.

8.4 Contingency Plans

If the drone is not able to complete a mission, the drone either returns to base, or finds the safest place to land. A return to base is the preferred contingency plan, but in the case of an emergency landing the drone uses its remaining systems to find the nearest place with the least amount of people to land. Recovery teams then respond to a location signal sent by the drone to receive it and process the incident.

8.5 Parachute System

In the case of unrecoverable system failure, a parachute will be deployed in order to safely return the drone to the ground. Currently available UAS parachute solutions, such as Safe2Ditch Autonomous Crash Management (NASA, 2018), ParaZero Drone Safety Solutions (Parazero, 2019), and Mars Auto Deploying Parachutes (Mars Parachutes, 2019), are all effective crash prevention methods, but they are all expensive, heavy, or power intensive. These significant restrictions influenced our decision to develop our own custom parachute solution drawing inspiration from available systems, while significantly reducing cost, and allowing us to scale parachutes to the size of our UAS.

There were multiple necessary criteria our parachute system would have to meet in order for us to consider it a safe solution to a total power loss. Our total parachute solution needs to be able to support the weight of the UAS, the system must know when to and be able to deploy

without electricity, and the system must be light, reusable, and cost effective. Based on the Mars parachute numbers (Mars Parachutes, 2019) we found that in order to meet the strength requirements, we require four parachutes about 130 inches in diameter. These provide about 27 pounds up lift and weigh about 0.8 pounds each. Each parachute is housed within an 8 inch by 3.5 inch diameter cylindrical capsule. Each capsule, made of polycarbonate with aluminum fasteners adds about 0.25 pounds per parachute, bringing the parachute system to a total of about 4.2 pounds.

With safety and redundancy in mind, there are two ways in which the parachutes can be triggered in the event of a system failure. The first mode is a mechanical or systems failure, for example one or more motors or sensors malfunction, or aren't responding to input from the computer. In this scenario, the computer's IMU predictions will not match measured accelerations, or the computer will detect a lack of input from the cameras, or receive a damage signal from a critical subset of motors. This information will qualify as a failure, and will prompt the computer to deploy the parachutes, bringing the UAS safely to the ground. The second triggering mechanism occurs during a total UAS power loss. Each UAS is equipped with a 9 volt battery backup deployment system, which is wired in parallel with the main computer like a dead man's switch and will deploy parachutes if the computer loses power.

This system, consisting of multiple parachutes with multiple ways to trigger them based on the mayday scenario, will be sufficient to prevent any injury to persons or damage to property in the event of a mechanical or system failure. These parachutes are reusable and provide ample resistance to slow the UAS descent significantly and efficiently. Additionally, due to the manner of the triggering methods, the parachutes will launch as soon as an issue is detected. Rather than the UAS first troubleshooting or attempting to fix whatever issue it detects, the parachutes

deploy at the earliest possible moment in failure, giving them plenty of time to fully deploy and not allowing the UAS to free-fall for any extended period before deployment.

9. Conclusion

Corvus is the first step in expanding the variety and capabilities of civilian UAV drones. The VTOL capabilities of Corvus ensure that it is able to take advantage of both traditional aircraft and helicopter capabilities as needed. Unlike most traditional civilian UAVs, this capability also ensures that Corvus is able to better fly in adverse weather conditions and at higher speeds, while still retaining fine omnidirectional mobility for landing and takeoff. The presence of redundant systems, reinforced structure, and parachutes ensures that Corvus is reliable and safe to those around it under any circumstances. The fully autonomous nature of Corvus serves to take human error out of the equation. No trained pilot would be required to operate Corvus, and Corvus itself will have faster response time and decision making than a human. The Corvus drone design presents an entirely new class of drone to meet the needs of logistics companies in expanding the versatility of their business operations. The speed and cost effectiveness of Corvus gives consumers the ability to receive their packages rapidly and inexpensively, more so than all existing delivery methods. Corvus also facilitates the savings of billions of dollars over existing urban transportation methods. The revolutionary design of Corvus will enable the evolution of the transportation industry into one fitting the next millennium.

References

National Aeronautic and Space Administration, "2019 – 2020 NASA Aeronautics University Design Challenge", Washington D.C., September 2019, https://aero.larc.nasa.gov/files/2019/09/NASA-Aeronautics-University-Design-Challenge-2019-2020-revA1.pdf

FAA. (2020, April 3). General Requirements for Certification. Retrieved May 3, 2020, from https://www.faa.gov/licenses_certificates/airline_certification/135_certification/general_req/

WingCopter. (2020). *Technical Details, Wingcopter 178 Heavy Lift*.

Schlachter, F., "Has the Battery Bubble Burst?," *APS Physics* Available: https://www.aps.org/publications/apsnews/201208/backpage.cfm.

Depron Foam. (n.d.). *Depron for Modeling.* http://depronfoam.com/products/

Federal Aviation Administration, "Certified Remote Pilots, Including Commercial Operators", Washington D.C., August 2019, https://www.faa.gov/uas/commercial_operators/

Federal Aviation Administration, "Waiver Trend Analysis", Washington D.C., August 2019, https://www.faa.gov/uas/commercial_operators/part_107_waivers/waiver_trend_analysis/

Lennon, A. (1996). *Basics of R/C model aircraft design: Practical techniques for building better models*. Air Age Incorporated.

Rios, J., & Boyle, A. (2020, April 24). NASA UTM. Retrieved from https://utm.arc.nasa.gov/index.shtml

M. Safarabadi (2018, August, 21). Parametric Flat Top Conveyor (Online). Available: https://grabcad.com/library/parametric-flat-top-conveyor-1

National Aeronautics and Space Administration (2018). Safe2Ditch Technology (Online). Available: https://technology.nasa.gov/patent/LAR-TOPS-243

Parazero Drone Safety Systems (2019). Professional Kit (Online) Available: https://parazero.com/products/astm-professional-kit/

Mars Parachutes (2019). Mars 120 V2 (Online) Available: https://www.marsparachutes.com/product/mars-120-v2/

Mad Components. (Mad M10 Ipe- 150kv High Efficient Brushless Motor For Paramotor and Paraglider). *Mad Components*. Retrieved from https://mad-motor.com/product/mad-m10-150kv-paramotor-version/

Drone Omega. (The Beginner's Guide To Drone Motor Essentials). *Drone Omega.* Retrieved from https://www.droneomega.com/drone-motor-essentials/

Gur, Ohad & Rosen, Aviv. (2009). Optimizing Electric Propulsion Systems for Unmanned Aerial Vehicles. Journal of Aircraft - J AIRCRAFT. 46. 1340-1353. 10.2514/1.41027.

Ryan. (2016, June 11). Torque vs Horsepower. Retrieved May 7, 2020, from https://www.radiocontrolinfo.com/torque-vs-horsepower/

Dronelife staff. (2019, November 7). DRONEII: The Drone Delivery Market Map. *DRONELIFE*. https://dronelife.com/2019/11/07/droneii-the-drone-delivery-market-map/

A Sample Commercial Drone Delivery Business Plan Template | ProfitableVenture. (n.d.). Retrieved April 2, 2020, from https://www.profitableventure.com/commercial-drone-delivery-business-plan/

$150 million Amazon fulfillment center near Grand Rapids will be built on fast-paced 22-week schedule. (n.d.). Building Design + Construction. Retrieved May 6, 2020, from https://www.bdcnetwork.com/150-million-amazon-fulfillment-center-near-grand-rapids-will-be-built-fast-paced-22-week-schedule

Keeney, T., & Analyst, A. R. K. (2015, May 5). *Drone Delivery: How Can Amazon Charge $1 for Drone Delivery?* ARK Investment Management. https://ark-invest.com/research/drone-delivery-amazon

Drone Delivery: Amazon Drone Delivery Program could... (2015, December 1). ARK Invest. https://ark-invest.com/analyst-research/amazon-drone-delivery/

How much Does it Cost to Build a Warehouse? Online Prices & Quotes. (n.d.). BuildingGuide | Steel Buildings | America. Retrieved May 6, 2020, from https://www.buildingsguide.com/blog/planning-steel-warehouse-building/

Small Package Sorting System Performance | USPS Office of Inspector General. (n.d.). Retrieved May 6, 2020, from https://www.uspsoig.gov/document/small-package-sorting-system-performance

The economics of Amazon's delivery drones « RobotEnomics. (n.d.). Retrieved May 6, 2020, from https://robotonomics.wordpress.com/2014/06/17/the-economics-of-amazons-delivery-drones/

Sudbury, A. W., & Hutchinson, E. B. (n.d.). *A COST ANALYSIS OF AMAZON PRIME AIR (DRONE DELIVERY)*. 12.

Unmanned Aircraft Systems Repairer Salaries in the United States. (n.d.). Indeed.Com. Retrieved May 7, 2020, from https://www.indeed.com/salaries/unmanned-aircraft-systems-repairer-Salaries

EIA - Electricity Data. (n.d.). Retrieved May 6, 2020, from https://www.eia.gov/electricity/monthly/epm_table_grapher.php?t=epmt_5_6_a

Jenkins, D., Vasigh, B., Oster, C., and Larsen, T., Forecast of the Commercial UAS Package Delivery Market, Embry-Riddle Aeronautical University, 2017.

Start a Drone Business: Ideas, Plans & Opportunities in 2020—Business Insider. (n.d.). Retrieved April 2, 2020, from https://www.businessinsider.com/start-drone-business-model

Amazon: Shipping costs 2019. (n.d.). Statista. Retrieved May 7, 2020, from https://www.statista.com/statistics/806498/amazon-shipping-costs/

Making the business case for drone delivery. (2018, March 16). Fleet Owner. https://www.fleetowner.com/technology/article/21702124/making-the-business-case-for-drone-delivery

NASA. (2018). Urban Air Mobility (Uam) Market Study.

Willcox, K. (2004, 19). Aircraft Systems Engineering: Cost Analysis. Lecture, MIT. Retrieved from http://ocw.mit.edu/courses/aeronautics-and-astronautics/16-885j-aircraft-systemsengineeringfall-2004/lecture-notes/pres_willcox.pdf

Drummond, C., & Yang, C. (n.d.). *Reverse-Engineering Costs: How much will a Prognostic Algorithm save?* 4.

Sonar System. (n.d.). Retrieved from https://www.sciencedirect.com/topics/engineering/sonar-system

Appendix

Appendix A

```
%STABILITY FOR

%%Aerodynamic center is usually localated at c/4 from the leading edge (c:
%%chord length)
%Mcg: Pitching moment (About Center of gravity)
%%Xcg: distance from the leading edge to cg
%%Xacw: distance from leading edge to aerodynamic center
%****** POSITIVE MOMENT IS TAKEN TO BE CLOCKWISE**********
%Assumption: Small angle of attach (alpha),
%Cl=a*alpha over most of the range of angle of attack (linear region)
%*Moment coeff about the ac of a camber wing is negative*
%iw: Angle between the fuselage reference line % and inclination of the wing
%Front wing: w subscript (CH)
%Back wing: t subscripts (FX 63-137)
%lENGTH FUSELAGE:62 IN


%*****ENTER VALUES*********
%LOCATION OF CG MEASURED FROM THE FORE TIP OF FUSELAGE(FT)
CGlocation=25/12; % (ft)
%HORIZONTAL DISTANCE FROM FORE TIP OF FUSELAGE TO LEADING EDGE OF FORE WING
WLocation=5.46/12; % (ft)WLocation=5.46/12
%HORIZONTAL DISTANCE FROM FORE TIP OF FUSELAGE TO LEADING EDGE OF AFT WING
TLocation=42.982/12; % (ft)
%FORE WING CHORD LENGTH
chordW=12/12;% (ft)
%AFT WING CHORD LENGTH
chordT=16/12;%(ft)
%FORE WING WING SPAN
wingSpanW=84/12;%(ft)
%AFT WING SPAN
wingSpanT=100/12;%(ft)
%Distance between front wing AC and CG in vertical direction(ft) (positive direction of z is downwards)
zCG = -1;

Zw=2.708/12 + zCG/12 ; %2.708/12
%Distance between back wing AC and CG in vertical direction(ft)
Zt=-1.392/12 - zCG/12;
%density
rho=0.002378;%Density at sea level
%Velocity
v=102.667; %air speed in ft/s (70 mph=102.667 ft/s)
```

```
%**********Given Parameters for the specific wings***************
%WIDTH FUSELAGE
WidthFuselage=10/12;
Sw=(wingSpanW-WidthFuselage)*chordW; %**Reference area front wing(ft^2)*
St=(wingSpanT-WidthFuselage)*chordT; %**Reference Area back wing*
Aw0=0.0945; %**Slope lift front wing (2 dimensional) (1/deg)Aw0=0.108
At0=0.1025; %**Slope lift back wing (2 dimensional) (1/deg) At0=0.11
iw=1.5; %$$Angle between the fuselage reference line and inclination of the front wing (degrees) ***ASSUMED***
it=.2; %$$Angle between the fuselage reference line and inclination of the back wing (degrees)  ***ASSUMED***
momW= 20.8 ;    %moment of front wing in lbf-ft
CmacW =-momW/(0.5*rho*v^2*Sw*chordW); %Moment coeff about the ac front wing    eppler 214 = -.0787

%my analysis shows moments don't really matter too much
MomT=64.26;%Moment of back wing in lbf-ft
CmacT=-.1899; % -MomT/(0.5*rho*v^2*St*chordT); %Moment coeff about the ac back wing
XbarAC=0.25; %Location Aero Center measured from leading edge divided by Front wing (FW) chord length
%****
XbarCG=(CGlocation-WLocation)/chordW; %Location of cg measured from the wing leading edge divided by FW chord length ***ASSUMED***


alphaLift0W=-11;%alphaLift0W=-4.5*Zero-Lift Angle of attack of Front wing (degrees)(zero if symmetric)

%this has 0L of selig
alphaLift0T=-7.75; %Zero-Lift Angle of attack of Back wing (degrees)(zero if symmetric)
ARw=wingSpanW/chordW; %*Aspect ratio Front Wing
ARt=wingSpanT/chordT; %*Aspect ratio Back Wing

%oswald has low impact
ew=0.83;%Oswald efficiency number front wing  ***ASSUMED*** COULDN'T FIND VALUE
et=0.835;%Oswald efficiency number back wing   ***ASSUMED***
lt=TLocation+.25*chordT-CGlocation;%Horizontal distance from CG to AC of Back wing (ft) ***ASSUMED .25 chord length for AC***
```

```
%*************Angle of attack variable (sweep)***********
alphaW=0:.01:10; %Angle of attack vector (degrees)

%************Define Variables to simplify************
%Turn Alpha into radians
alphaW=alphaW./57.3;
%Turn Aw0 into 1/radians
Aw0=Aw0*57.3;
%Turn At0 into 1/radians
At0=At0*57.3;
%Turn iw into radians
iw=iw/57.3;
%Turn it into radians
it=it/57.3;
%Turn alphaLift0W into radians
alphaLift0W=alphaLift0W/57.3;
%Turn alphaLift0T into radians
alphaLift0T=alphaLift0T/57.3;

%Dimentionalize Zw
ZbarW=Zw/chordW;

aw=Aw0/(1+Aw0/(pi*ew*ARw));%Finite front wing lift slope(1/rad)
at=At0/(1+At0/(pi*et*ARt));%Finite back wing lift slope
%***Calculate lift coefficients
Cl0w=aw*abs(alphaLift0W); % Lift coeff at zero angle of attack front wing
%Then CLw is
CLw= (Cl0w+aw.*alphaW); % cfd says .78 on front wing at 4 degrees, this says 1.09

%From finite wing theory
eps0=(2*Cl0w)/(pi*ARw);
de=(2*aw)/(pi*ARw);

%***Define Angle of attack of back wing in terms of front wing
alphaT=alphaW+(it-iw)-(eps0+de.*alphaW);
%now
Cl0t=at*abs(alphaLift0T);% Lift coeff at zero angle of attack back wing
CLt= (Cl0t+at.*alphaT); % cfd says .40, this says .343
```

```
%*****Define Moment coefficient for front wing****
McCGw=CLw.*(XbarCG-XbarAC+ZbarW.*(alphaW-iw))+CmacW;

%*****Define Moment coefficient for rear wing****
McCGt=-((St.*CLt)/(Sw*chordW)).*(lt+Zw.*(alphaT-it)) + CmacT;


%***************PITCHING MOMENT AIRCRAFT***************
CmPitch=McCGw+McCGt;



%Dont forget to multiply alpha by 180/pi
%to get the angle in degrees
alphaDegrees=alphaW.*57.3;
figure
plot(alphaDegrees,CmPitch,'r')
hold on
plot(alphaDegrees,McCGw,'m--')
plot(alphaDegrees,McCGt,'g--')
plot(alphaDegrees,zeros(1,length(alphaDegrees)),'k')
legend('Aircraft', 'Fore Wing (CH 10-48-13)','Aft Wing (FX 67-137)')
hold off
title("Pitching moment")
xlabel("Angle of Attack")
ylabel("Cm_c_g")
```

Appendix B

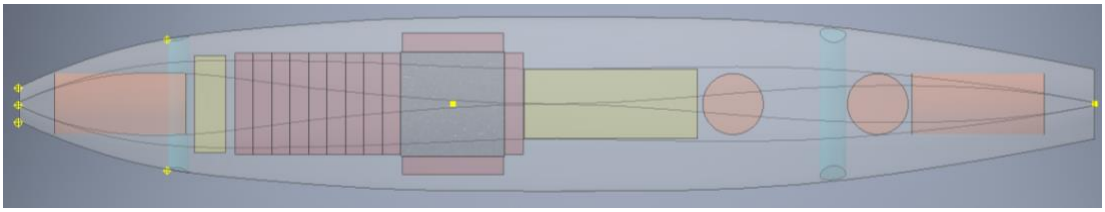

Top view of the interior of the fuselage

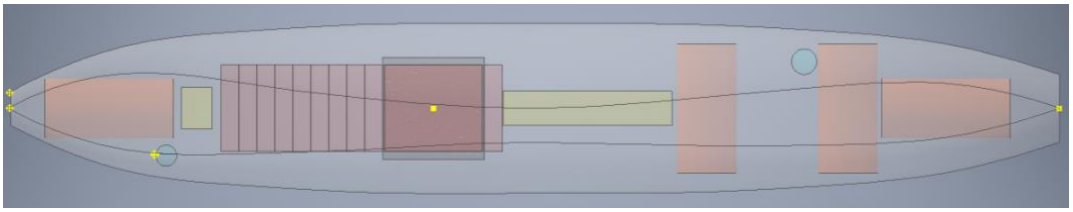

Right view of the interior of the fuselage

Appendix C

Parameter	Specification		
Material:	Extruded Polystyrene foam, formed as sheets		
Thickness:	3mm *(± 10%)*	6mm *(±8%)*	9mm (±8%)
Colour:	White	White	White
Size:	1250x800mm (±4mm x ±2mm)	1250x800mm (±4mm x ±2mm)	1000x700mm (±4mm x ±2mm)
Full box qty:	40 sheets	20 sheets	13 sheets
Density:	33kg/m³ (±10%)	28kg/m³ (±10%)	28kg/m³ (±10%)
Weight:	Ca. 100g/m² *(± 10%)*	Ca. 168g/m² *(± 10%)*	Ca. 252g/m² *(± 10%)*
Compressive Strength: (with 10% compression)	>100kPa	>100kPA	>120kPa
Absorption of water:	< 0.1 Vol%	< 0.1 Vol%	< 0.1 Vol%
Application Temperature:	-60°C / +70°C	-60°C / +70°C	-60°C / +70°C
Fire Classification:	F	F	F

Appendix D

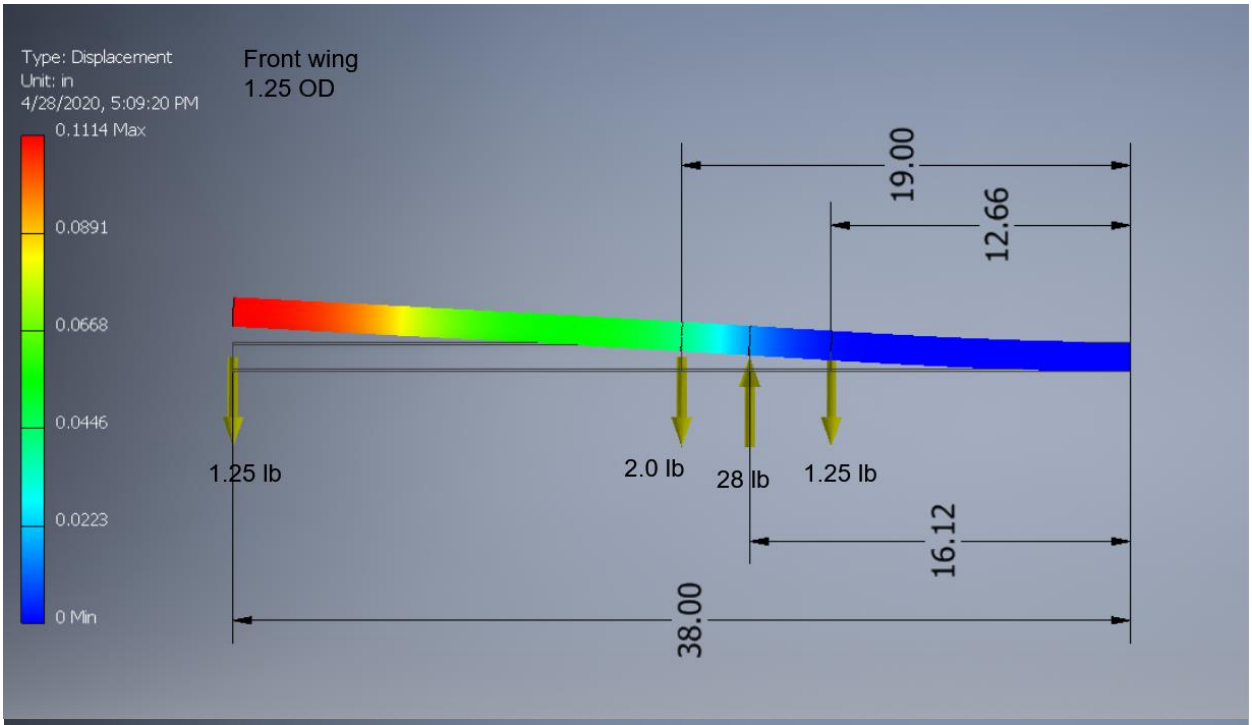
Type: Displacement
Unit: in
4/28/2020, 5:09:20 PM
0.1114 Max
0.0891
0.0668
0.0446
0.0223
0 Min
Front wing
1.25 OD
19.00
12.66
1.25 lb
2.0 lb
28 lb
1.25 lb
16.12
38.00

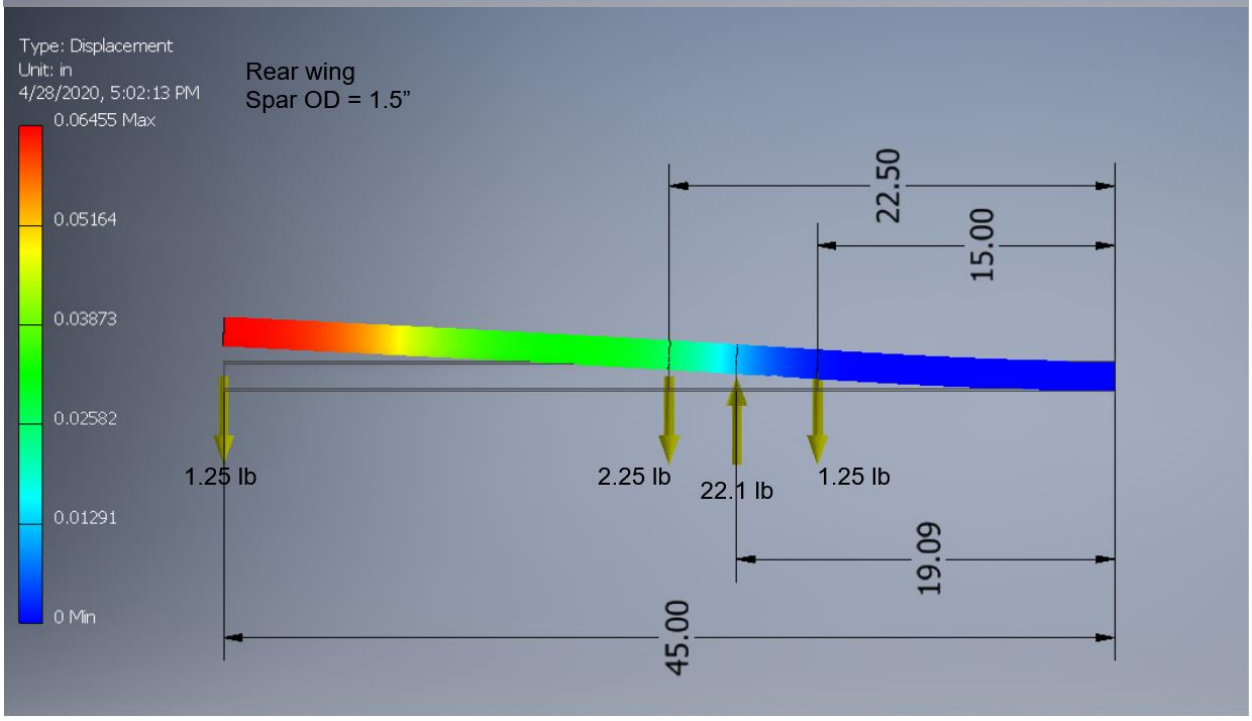
Type: Displacement
Unit: in
4/28/2020, 5:02:13 PM
0.06455 Max
0.05164
0.03873
0.02582
0.01291
0 Min
Rear wing
Spar OD = 1.5”
22.50
15.00
1.25 lb
2.25 lb
22.1 lb
1.25 lb
19.09
45.00

Appendix E

Symmetric airfoil. $\alpha_{max} = 15°$ $C_{L_{max}} = 1.2363$

$L = C_L \frac{1}{2} \rho V^2 A$

$\rho = 0.002378$ slug/ft³

$V = 102.67$ ft/s

$A = (height)(width)$

$width = 10/12$ ft

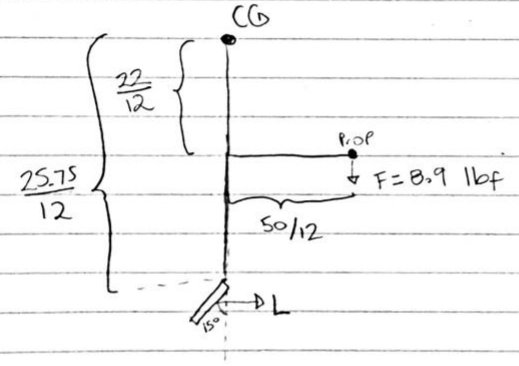

NACA 0012

Assumption: Drag will be negligible

$\circlearrowleft + \sum M_{CG} = 0 \Rightarrow \sum M_{CG} = (8.9)(50/12) - (L)(25/12) = 0$

$L = \frac{(8.9)(50/12)}{25.75/12}$

$\rightarrow C_L \frac{1}{2} \rho V^2 (HW) = \frac{(8.9)(50)}{25.75/12}$

$H = \frac{(8.9)(50)}{(25.75)} \quad \frac{2}{C_L \rho V^2 W}$

$H = 1.39$ ft $\rightarrow$ **H = 16 in**

Appendix F

Table of Component Weights and Locations

Component	Weight (lbs)	Location (in)
Battery	31.75	19.457
Fuselage	9.3	31
Wings	5.41	29.2
Wing Spars	4.1	28.1
Vertical Stabilizer	1.35	52
DAA Hardware	5.6	6
AI Unit	7.72	34.1
Piccolo Elite	0.44	11
Package	5	25
Motors	10.05	24.55
Servos	4.7	28.1
Parachute	7.67	37.7
Propellers	4	24.55
Wiring	3	31
Landing Struts	2	31
Total	**102.09**	

Appendix G

Components	Model	Power Consumption Estimation	Mass
Servos for front wing (1)	DA 30	36.4W (Standby: 1.12 W)	0.67kg
Servos for aft wing (1)	DA 30 HT	56W (Standby: 1.12W)	1.1kg
Servos for motors (2)	DA 26	44.8W	0.54kg
Control Surface Servos (5)	Hobby Porter WP26	18.5W	0.375kg